NASA TECHNICAL NOTE

NASA TN D-4275

NASA TN D-4275

WATER PRESSURES AND ACCELERATIONS DURING LANDING OF A DYNAMIC MODEL OF THE APOLLO SPACECRAFT WITH A DEPLOYED-HEAT-SHIELD IMPACT-ATTENUATION SYSTEM

by Sandy M. Stubbs

Langley Research Center
Langley Station, Hampton, Va.

NATIONAL AERONAUTICS AND SPACE ADMINISTRATION • WASHINGTON, D. C. • MARCH 1968

NASA TN D-4275

WATER PRESSURES AND ACCELERATIONS DURING LANDING OF A DYNAMIC MODEL OF THE APOLLO SPACECRAFT WITH A DEPLOYED-HEAT-SHIELD IMPACT-ATTENUATION SYSTEM

By Sandy M. Stubbs

Langley Research Center
Langley Station, Hampton, Va.

Technical Film Supplement L-980 available on request.

NATIONAL AERONAUTICS AND SPACE ADMINISTRATION

For sale by the Clearinghouse for Federal Scientific and Technical Information
Springfield, Virginia 22151 – CFSTI price $3.00

WATER PRESSURES AND ACCELERATIONS DURING LANDING OF A DYNAMIC MODEL OF THE APOLLO SPACECRAFT WITH A DEPLOYED-HEAT-SHIELD IMPACT-ATTENUATION SYSTEM

By Sandy M. Stubbs
Langley Research Center

SUMMARY

An experimental investigation was made to determine impact water pressures, accelerations, and landing dynamics of a 1/4-scale model of the command module of the Apollo spacecraft with a deployed heat shield for impact attenuation. The landing system consisted of four vertically oriented hydraulic struts and six horizontally mounted strain straps. A scaled-stiffness aft heat shield was used on the model to simulate the structural deflections of the full-scale heat shield. Landings were made at simulated vertical parachute-letdown velocities of approximately 30 ft/sec (9.1 m/sec) full scale. Horizontal velocities from 0 to 50 ft/sec (15 m/sec), full scale, were tested, and the pitch attitudes ranged from -33° to 11°. Roll attitudes were 0° and 180°, and yaw attitude was 0°.

The model investigation indicated that the maximum mean water pressure on sample panels of the spacecraft heat shield with an area of about 1.6 feet^2 $(0.15\ m^2)$, full scale, was approximately 165 psi $(1140\ kN/m^2)$. The maximum mean pressures on panels with areas of 1.9 feet^2 $(0.18\ m^2)$ and 10.9 feet^2 $(1.01\ m^2)$ were about 110 psi $(760\ kN/m^2)$. Pressures for 0° and 180° roll were similar. The maximum mean pressure at the time of maximum acceleration was approximately 18 psi $(120\ kN/m^2)$ for the deployed-heat-shield system compared with 50 psi $(340\ kN/m^2)$ for a passive landing system.

Maximum normal and longitudinal accelerations for the 0° roll condition were 25g and 6g, respectively $(1g = 9.8\ m/sec^2)$. Maximum positive and negative angular accelerations were about 95 and $-55\ rad/sec^2$. The vehicle with the deployed heat shield was stable for all conditions investigated.

INTRODUCTION

One of the many aspects of manned space flight being investigated by the National Aeronautics and Space Administration is the landing of a spacecraft upon its return to earth. Landing characteristics of various models of manned spacecraft are presented in references 1 to 4. The Apollo command module is currently being developed for a three-man lunar mission which includes an earth landing by parachute. The original landing

system design for the Apollo spacecraft called for a deployed aft heat shield with a primary landing medium of soil and a secondary landing medium of water. For various reasons, these criteria were changed after the development of the landing system was underway. The change was to a passive landing system, which does not require heat-shield deployment or braking rockets, with water as the primary landing medium and soil, the secondary.

Reference 5 presents water-pressure data for a model of the Apollo spacecraft with a passive landing system. The loads imposed on the heat shield during landing impact govern the design of the heat shield and its supporting structure. The present investigation was made to determine the impact water pressures and accelerations imposed on a 1/4-scale dynamic model of one version of the Apollo command module which used a deployed-heat-shield landing system and to determine whether the shock-absorber action between the heat shield and the main mass of the vehicle would result in lower impact water pressures and hence in lower aft heat-shield structural loads.

Tests were made on calm water at attitudes simulating a combination of vehicle oscillation under the parachute and wave slope. Vertical and horizontal velocities simulated parachute-letdown conditions. The investigation was conducted in the Langley impacting structures facility.

The units used for the physical quantities defined in this paper are given both in U.S. Customary Units and in the International System of Units (SI). (See ref. 6.) Appendix A presents factors relating these two systems of units. All test conditions and results are presented in full-scale values unless otherwise indicated.

DESCRIPTION OF MODEL

The model used in the investigation was a 1/4-scale dynamic model of the command module of the Apollo spacecraft with a deployed heat shield for landing-impact attenuation. The scale relationships between the model and full-scale spacecraft are listed in table I. Pertinent parameters of the spacecraft are given in table II.

The general arrangement of the model is shown in figure 1. Figure 2 shows the location of the landing-gear components. Photographs of the model are presented as figure 3. The model had an aluminum frame to which an outer skin of fiber glass and plastic, approximately 1/8 inch (0.32 cm) thick, model scale was attached. The bottom of the crew compartment was solidly filled with balsa wood to reduce structural vibrations. Mahogany blocks were inserted in the balsa wood to serve as accelerometer mounts.

The landing system consisted of four vertical hydraulic struts and six horizontal strain straps. (See fig. 2.) Photographs of the landing-gear components are presented

as figure 4. The assembled and disassembled vertical hydraulic strut is shown in figure 4(a). Details of the development of the hydraulic strut are reported in reference 7. The force characteristics of a single dynamically loaded strut are shown in figure 5. To obtain the typical force-time curve shown, an accelerometer was mounted on a 1.24-slug (18.1-kg) lead mass, which represented slightly more than one-fourth of the mass of the model, and dropped so that the velocity at impact with the hydraulic strut was 15 ft/sec (4.6 m/sec) model scale. The maximum force developed by the hydraulic strut was approximately 780 lbf (3.5 kN) model scale.

The horizontal strain straps (figs. 2 and 4(b)) are provided to limit rotation and shearing motions between the aft heat shield and the upper body. The strain straps were made of low-carbon nickel wire. The stress-strain characteristics of the wire are shown in figure 6. By using a yield stress of approximately 30 000 lbf/in^2 $(210\ MN/m^2)$, the front straps (four wires of 0.08-inch (0.20-cm) diameter) were designed to yield at a force of about 600 lbf (2.7 kN); the side straps (three wires), at a force of 450 lbf (2.0 kN); and the rear straps (two wires), at a force of 300 lbf (1.3 kN) model scale.

The model used in this investigation is the same as configuration 2 in reference 8 with the exception of the heat shield. The construction details of the heat shield used in the investigation are shown in figure 7. The heat shield used in this investigation has thinner fiber-glass face sheets than the heat shield reported in reference 8. The heat-shield stiffness was scaled from an early Apollo heat-shield structural design. (See ref. 7.) For the model, a sandwich construction was used with a core of styrene plastic foam covered on each side by two layers of glass cloth impregnated with an epoxy resin. Lead weights were distributed between the fiber-glass layers on 2-inch (5-cm) centers, model scale, to obtain proper inertial characteristics of the heat shield. The load-deflection curve of the heat shield used in the present investigation is presented in figure 8 along with a curve of the loading of a typical heat shield through its failure regime. The failure-regime data are presented to illustrate how the failures affect the force-deflection curve. The deflections were measured from the movement of the machine head. The deflection of the heat shield during water impact is relatively small compared with the stroke of approximately 3 inches (8 cm), model scale, provided by the vertical hydraulic struts.

The location of pressure transducers on the heat shield is shown in the sketch of the inside of the heat shield (fig. 9). The pressure transducers were arbitrarily numbered from 5 to 23. The corresponding instrumentation characteristics are presented in table III. To obtain mean pressures, defined in appendix B, from arbitrary circular panel areas labeled A to J, the pressure transducers were arranged in overlapping groups of three for each area as shown in figure 10. Panels A to E each represent an area of approximately 1.6 $feet^2$ $(0.15\ m^2)$ full scale. Panels F to J each represent an area of

1.9 feet^2 (0.18 m^2). Panels K and L are each made up of four smaller panels and represent an area of approximately 10.9 feet^2 (1.01 m^2) full scale. The panels are only areas defined for use in data analysis and are not structural elements.

APPARATUS AND PROCEDURE

Test Conditions

Tests were made on a calm fresh-water landing surface at simulated parachute-letdown velocities. The vertical velocity component varied from 28 to 31 ft/sec (8.5 to 9.4 m/sec), full scale, and the horizontal velocity component varied from 0 to 50 ft/sec (15 m/sec) full scale. Pitch attitudes ranged from -33° to 11°. Roll attitudes were 0° and 180°; yaw attitude was 0°. Figure 11 shows the model acceleration axes, flight path, force directions, and landing attitudes. The axes of the spacecraft are oriented the same as standard airplane axes with respect to the pilot. It should be noted, however, that the attitude of the spacecraft axes with respect to the landing surface is different from that of an airplane.

For this investigation the nominal attitude for spacecraft descent under the parachute was -10°. This angle was selected on the basis of results of a previous investigation (ref. 8) which indicated -10° as the most stable attitude for landings on a hard surface. A variation in landing attitude from -33° to 11° was tested to include the swing (up to ±8°) of the spacecraft about the -10° attitude under the letdown parachute in addition to possible wave slopes (up to ±8°).

Launch Procedure and Apparatus

The launch procedure is illustrated in figure 12. A pendulum was released from a predetermined height to produce the desired horizontal velocity. The model was released at the lowest point of the swing, and the free fall gave the desired vertical velocity. The launch apparatus is shown in figure 13.

Instrumentation

Normal and longitudinal accelerations were measured at the center of gravity of the vehicle with linear strain-gage accelerometers. Angular (pitch) accelerations were measured with matched pairs of linear accelerometers suitably connected electrically. Impact water pressures were measured with strain-gage pressure transducers. The response characteristics of the transducers and related recording equipment (amplifiers, oscillographs, and galvanometers) are shown in table III. The pressure transducers had a diaphragm 0.50 inch (1.3 cm) in diameter and were flush mounted in the heat shield. A thin plastic tape was placed over the diaphragm of each transducer to insulate it from the

temperature shock that occurs upon contact with the water. It was determined that the tape did not affect the pressure values but acted only as an insulator. Signals from all transducers were transmitted through trailing cables to the recording equipment.

Motion pictures were made to record the landing behavior of the model.

RESULTS AND DISCUSSION

The data obtained in the investigation are presented in table IV. All the values presented in this section are full scale unless otherwise indicated.

Motion-picture film supplement L-980 showing landing tests of the 1/4-scale model of the Apollo command module has been prepared and is available on loan. A request card form and a description of the film are included at the back of this paper.

Accelerations

Typical oscillograph records obtained at pitch attitudes of -29°, -9°, and 11° are shown in figure 14. The vertical and horizontal velocities for the data shown were each approximately 30 ft/sec (9.1 m/sec). The roll and yaw attitudes were 0°. The dashed lines are fairings of the accelerometer and pressure-transducer traces. Data presented in table IV and in the figures were obtained from similar fairings.

The normal, longitudinal, and angular acceleration traces, shown in figure 14(a) for a pitch attitude of -29°, indicate gradual onset rates of acceleration. At this attitude low accelerations result because the sharp lower edge is the first part of the vehicle to contact the water surface. When the flatter bottom surface of the heat shield contacts the water first (at attitudes of -9° and 11°) accelerations are increased as indicated in figures 14(b) and (c).

Accelerations obtained in the investigation are plotted in figure 15(a) for 0° roll and in figure 15(b) for 180° roll. The maximum normal acceleration at 0° roll was 25g at a -2° landing attitude $\left(1g = 9.8\ m/sec^2\right)$. Maximum longitudinal accelerations were 6g. Angular accelerations for some runs had both positive and negative peaks. (See fig. 14(c).) The maximum positive and negative angular accelerations were approximately 95 and -55 rad/sec^2.

The maximum normal and longitudinal accelerations for the 180° roll condition (fig. 15(b)) were 19g and 6g, respectively, as compared with 38g and 7.5g, respectively, for the passive landing system presented in reference 5. The maximum positive and negative angular accelerations were approximately 70 and -90 rad/sec^2.

Pressure Data

Panel pressures.- Two methods of interpreting the data for the individual panels to obtain the mean pressure are discussed in appendix B. Briefly, one method is to average the three transducer-pressure values at the time the last transducer of a panel reaches its peak. The other method is to obtain an incremental summation of a pressure diagram made for a given panel by plotting the three transducer values and fairing a line through the plotted points. Both methods were used in this investigation. The data from the incremental method are indicated by a footnote in table IV. The incremental summation of the panel pressure is the more accurate of the two methods of analysis but is a great deal more time consuming. Because of other sources of error, such as inaccuracies in instrumentation response, heat-shield flexibility effect, and water-surface irregularities, a simple averaging on most panels was considered adequate.

The pressure values for panels K and L (fig. 10) were obtained by the method of averaging all transducer values at the time the last transducer in the panel reaches its peak value.

Data points and faired curves for maximum mean pressures on panels A to F at 0° roll are shown in figure 16(a). Figure 16(b) shows similar data for panels G to L. Figure 17 presents panel-pressure data obtained at a 180° roll attitude. The effect of horizontal velocity was neglected in fairing the data points since only trends were being studied. Only the faired curves are presented in figures 18 and 19. These are considered to be more representative of the pressures on the panels than the individual data points plotted in figures 16 and 17.

Figures 18 and 19 are each divided into three parts for comparisons of the three panel sizes considered in the investigation. Figure 18 shows faired curves for the 0° roll condition. Figure 18(a) shows data for panels A to E $\left(1.6 \text{ feet}^2 \left(0.15 \text{ m}^2\right)\right)$. The mean pressure on panel A increases from about 10 psi $\left(70 \text{ kN/m}^2\right)$ at an attitude of -30° to 165 psi $\left(1140 \text{ kN/m}^2\right)$ at a -19° attitude, then decreases to 20 psi $\left(140 \text{ kN/m}^2\right)$ at -5° and drops only slightly between -5° and 10°. The impact water pressure experienced by a panel is dependent on the impacting velocity and the angle at which the panel strikes the water. Panel A contacts the water at a near zero, or flat, attitude when the vehicle is at a -19° attitude. (See fig. 10.) For higher negative angles than -19°, panel A is the first panel to contact the water and thus should have higher pressures than the other panels, but the angle at which it strikes the water is increasing so that at -30° the panel is at a 11° angle with respect to the water surface. The increasing contact angle of the panel results in decreasing pressures for landing attitudes from -19° to -30° and also for attitudes from -19° to 11°. Panel B impacts the water at a flat angle for a -13° landing attitude; panel C, -5°; panel D, 1°; and panel E, 9°. (See fig. 10.) The maximum mean panel

pressures for these panels all occur at or near their individual flat impact angles. The maximum mean pressure varies from about 115 psi $(790\ kN/m^2)$ for panel E to 165 psi $(1140\ kN/m^2)$ for panel A.

The faired data curves for panels F to J $(1.9\ feet^2\ (0.18\ m^2))$ are shown in figure 18(b). Panels F and I are equidistant from the Y and Z axes of the model, and since the impact points are along the Z-axis (0^o yaw), these panels should have similar pressures for any given attitude. The same is true for panels G and H. Panels F to J at no time impacted the water at a flat attitude, and thus pressures for these panels would be expected to be lower than the pressures for the panels lying along the Z-axis. Panel J experienced lower pressures than the other panels because it is farthest from the Z-axis. The maximum mean pressure for panels F and I is about 110 psi $(760\ kN/m^2)$. The maximum mean pressure for panels G and H is approximately 120 psi $(830\ kN/m^2)$.

The faired data curves for panels K and L $(10.9\ feet^2\ (1.01\ m2))$ are shown in figure 18(c). There are still substantial pressures on these much larger panels. The maximum mean pressure for both panels is approximately 110 psi $(760\ kN/m^2)$.

The faired data curves for the 180^o roll condition (fig. 19) are similar in shape and magnitude to the curves obtained for the 0^o roll condition. At the high negative angles of the tests, the pressures are consistently higher for the 180^o roll condition than for 0^o roll.

Pressure at time of maximum acceleration.- The mean pressure over the wetted area at the time of maximum acceleration was determined in addition to the panel pressures. The method of analyzing the data is presented in appendix B. Briefly, the analysis used the wetted area at the time of maximum acceleration and the forces obtained from the resultant acceleration. The force obtained from the accelerometer data was divided by the wetted area. The wetted area was determined from the number of transducers that had experienced their maximum pressures. The mean pressure at the time of maximum acceleration is shown in figure 20. The solid line faired through the data indicates mean pressures ranging from about 5 psi $(30\ kN/m^2)$ to approximately 18 psi $(120\ kN/m^2)$ for both roll attitudes. Also shown in figure 20, as a dashed line, is the mean pressure for the passive landing system presented in reference 5. Mean pressures for the passive landing system varied from about 20 psi $(140\ kN/m^2)$ to 50 psi $(340\ kN/m^2)$. A comparison of the wetted areas for the two systems at the time of maximum acceleration is shown in figure 21. The data points and the solid-line fairing show the wetted areas for the current investigation. The dashed line shows the wetted areas for the passive system obtained from the data presented in reference 5. The larger wetted areas and lower forces (accelerations) for the deployed-heat-shield model as opposed to the smaller wetted area and higher forces (see ref. 5) for the passive-system model result in the lower mean pressures experienced by the deployed-heat-shield model presented in figure 20.

Landing Stability

The vehicle with the deployed heat shield was stable for all conditions investigated. That is, it came to rest in an upright position. The flotation characteristics for this vehicle are similar to those for the vehicle of reference 8. The vehicle floats stably in an approximately upright position and in a near-inverted position.

CONCLUDING REMARKS

A landing investigation has been made of a 1/4-scale dynamic model of the command module of the Apollo spacecraft having a deployed heat shield with four hydraulic struts and six strain straps for impact attenuation. The landing-impact water pressures, accelerations, and landing dynamics of the test model were determined.

The model investigation indicated that the maximum mean water pressure on sample panels of the spacecraft heat shield with areas of about 1.6 feet^2 $(0.15\ m^2)$ was approximately 165 psi $(1140\ kN/m^2)$ at a vertical velocity of 30 ft/sec (9.1 m/sec) full scale. The maximum mean pressures on panels with areas of 1.9 feet^2 $(0.18\ m^2)$ and 10.9 feet^2 $(1.01\ m^2)$ were about 110 psi $(760\ kN/m^2)$. Pressures for 0^o and 180^o roll were similar. The maximum mean pressure at the time of maximum acceleration was approximately 18 psi $(120\ kN/m^2)$ for the deployed-heat-shield system compared with 50 psi $(340\ kN/m^2)$ for a passive landing system.

Maximum normal and longitudinal accelerations for the 0^o roll condition were 25g and 6g, respectively. Maximum positive and negative angular accelerations were about 95 and -55 rad/sec^2. The vehicle with the deployed heat shield was stable for all conditions investigated.

Langley Research Center,
National Aeronautics and Space Administration,
Langley Station, Hampton, Va., November 14, 1967,
124-08-04-06-23.

APPENDIX A

CONVERSION OF U.S. CUSTOMARY UNITS TO SI UNITS

The International System of Units (SI) was adopted by the Eleventh General Conference on Weights and Measures, Paris, October 1960, in Resolution No. 12 (ref. 6). Conversion factors for the units used herein are given in the following table:

Physical quantity	U.S. Customary Unit	Conversion factor (*)	SI Unit
Length	in.	0.0254	meters (m)
Area	in^2	6.4516×10^{-4}	$meters^2$ (m^2)
Mass	slug	14.5939	kilograms (kg)
Moment of inertia . . .	$slug\text{-}ft^2$	1.35582	$kilogram\text{-}meters^2$ $(kg\text{-}m^2)$
Velocity	ft/sec	0.3048	meters/second (m/sec)
Linear acceleration . .	ft/sec^2	0.3048	$meters/second^2$ (m/sec^2)
Force	lbf	4.448	newtons (N)
Stress, Pressure	$psi = lbf/in^2$	6.89×10^3	$newtons/meter^2$ (N/m^2)

*Multiply value given in U.S. Customary Unit by conversion factor to obtain equivalent value in SI Unit.

Prefixes to indicate multiples of units are as follows:

Prefix	Multiple
milli (m)	10^{-3}
centi (c)	10^{-2}
kilo (k)	10^3
mega (M)	10^6

APPENDIX B

METHODS OF ANALYZING THE PRESSURE DATA

The approximate mean pressures presented in this report refer to the sample panel areas shown in figure 10. The theoretical mean pressure is defined as the integration of the pressure over any one of the panels divided by the area of the panel; that is,

$$p_m = \frac{\int p \, dA}{A}$$

where

p_m mean pressure

p local pressure

A panel area

This would ideally be the preferred method of obtaining the mean pressure; but because of the limited coverage available from the instrumentation, inaccuracies in reading the pressures, inaccuracies in instrumentation response, heat-shield flexibility, water-surface irregularities, and other considerations, the mean pressure was approximated by one of the following more simplified methods. One method used an incremental summation of pressure and the other used a simple arithmetic averaging of the three transducer values.

Figure 22 shows sketches of pressure distributions for panels A, B, and C drawn along the Z-axis. Only three transducers were used for each panel because of limited availability of instrumentation. The point of initial contact is shown and the direction of the water line in moving across the panel is indicated by the arrow passing through the center of each panel. All three pressure transducers (5, 6, and 7 for panel A) were read at the time the last of the three transducers reached its peak value. The position of the water line is shown for each panel at the time the three transducer values were simultaneously read. The three pressure values for each panel are shown plotted as a function of the projected distance between the transducers, and a dashed line indicates the fairing of the pressure diagram. The pressure diagram is considered to represent the pressures along the solid line passing through the center of each panel (A-A, B-B, and C-C). Furthermore, the mean pressure value obtained from the diagram is considered to approximate the mean pressure over the entire panel.

For panel B the diagram was divided into four equal increments a, b, c, and d, and the sum of the average values for the increments was divided by 4 to obtain the mean

pressure for the panel. In general, for panels that were located with respect to the point of initial contact so that two transducers were read when both were at or near their peak value, a diagram was made (shown for panel B), and the incremental method was used to obtain the mean pressure. For other panels (A and C are typical examples) a simple arithmetic average was used to approximate the mean pressure for the panel. The incremental method is a more accurate method of obtaining the mean pressure, but it is a great deal more time consuming, and because of other inaccuracies involved, a simple averaging was considered adequate for most panels.

The mean wetted-area pressure at the time of maximum acceleration was determined in addition to the panel pressures. The pressure transducers in this case were used only to determine the position of the water line at the time of maximum acceleration. The wetted area was then calculated by drawing the water line on a planform sketch of the heat shield and integrating with a planimeter. The mean wetted-area pressure $p_{m,wa}$ was obtained from

$$p_{m,wa} = \frac{F}{A_w}$$

where

F force, ma_r

A_w wetted area

m mass

a_r maximum resultant acceleration

It was difficult, however, to be sure of the exact time at which maximum acceleration was reached, especially for tests at the higher negative attitudes (fig. 15(a)). Therefore, the data presented for the mean wetted-area pressure at the time of maximum acceleration should be considered approximate.

REFERENCES

1. McGehee, John R.; Hathaway, Melvin E.; and Vaughan, Victor L., Jr.: Water-Landing Characteristics of a Reentry Capsule. NASA MEMO 5-23-59L, 1959.

2. Vaughan, Victor L., Jr.: Landing Characteristics and Flotation Properties of a Reentry Capsule. NASA TN D-653, 1961.

3. Stubbs, Sandy M.: Landing Characteristics of a Reentry Vehicle With a Passive Landing System for Impact Alleviation. NASA TN D-2035, 1964.

4. Thompson, William C.: Dynamic Model Investigation of the Landing Characteristics of a Manned Spacecraft. NASA TN D-2497, 1965.

5. Stubbs, Sandy M.: Dynamic Model Investigation of Water Pressures and Accelerations Encountered During Landings of the Apollo Spacecraft. NASA TN D-3980, 1967.

6. Mechtly, E. A.: The International System of Units – Physical Constants and Conversion Factors. NASA SP-7012, 1964.

7. Bennett, R. V.; and Koerner, F. W.: 1/4 Scale Apollo Impact Attenuation Model. Rept. No. NA62H-513, North Am. Aviation, Inc., Sept. 14, 1962.

8. Stubbs, Sandy M.: Landing Characteristics of the Apollo Spacecraft With Deployed-Heat-Shield Impact Attenuation Systems. NASA TN D-3059, 1966.

TABLE I.- SCALE RELATIONSHIPS

[λ = Scale of model = 1/4]

Quantity	Full-scale value	Scale factor	Model
Dynamic model:			
Length	l	λ	λl
Area	A	λ^2	$\lambda^2 A$
Mass	m	λ^3	$\lambda^3 m$
Moment of inertia	I	λ^5	$\lambda^5 I$
Time	t	$\sqrt{\lambda}$	$\sqrt{\lambda} t$
Speed	V	$\sqrt{\lambda}$	$\sqrt{\lambda} V$
Linear acceleration . . .	a	1	a
Angular acceleration . . .	α	λ^{-1}	$\lambda^{-1}\alpha$
Force	F	λ^3	$\lambda^3 F$
Pressure	p	λ	λp
Energy strap:			
Unit stress	σ	1	σ
Cross-sectional area[a] . .	A	λ^3	$\lambda^3 A$
Force	F	λ^3	$\lambda^3 F$

[a]For dynamic similarity it is convenient to keep linear acceleration 1:1 for model and full scale. Since the mass varies as the cube of the scale factor (λ^3), all applied forces must be varied by the same factor. A geometrically scaled energy strap would vary as λ^2; therefore, it is necessary to distort the cross-sectional area of the strap and vary it as λ^3.

TABLE II.- MEASURED PERTINENT PARAMETERS OF MODEL

Parameter	1/4-scale model		Full-scale vehicle	
Mass	4.36 slugs	63.7 kg	280 slugs	4080 kg
Moment of inertia (heat shield retracted):				
I_X (roll)	4.24 slug-ft^2	5.75 kg-m^2	4340 slug-ft^2	5880 kg-m^2
I_Y (pitch)	3.59 slug-ft^2	4.87 kg-m^2	3680 slug-ft^2	4990 kg-m^2
I_Z (yaw)	3.01 slug-ft^2	4.08 kg-m^2	3080 slug-ft^2	4180 kg-m^2
Body:				
Diameter	37.88 in.	0.962 m	151.50 in.	3.85 m
Height (heat shield retracted)	21.21 in.	0.539 m	84.84 in.	2.15 m
Spherical radius of heat shield	44.15 in.	1.121 m	176.60 in.	4.49 m

TABLE III.- INSTRUMENTATION CHARACTERISTICS

Accelerometer orientation	Range, g units	Natural frequency, cps	Damping, percent of critical damping	Limiting flat frequency of other recording equipment, cps
Normal (at vehicle c.g.)	±50	613	0.60	600
Longitudinal (at vehicle c.g.)	±50	633	.60	600
Angular (pitch)	±100	685	.65	600

Pressure transducer	Range		Approximate natural frequency in air, cps	Limiting flat frequency of other recording equipment, cps
	psi	kN/m^2		
5	100	689	11 000	5000
6	100	689	11 000	5000
7	100	689	11 000	5000
8	100	689	11 000	5000
9	100	689	11 000	5000
10	100	689	11 000	5000
11	100	689	11 000	5000
12	100	689	11 000	5000
13	100	689	11 000	5000
14	100	689	11 000	5000
15	150	1034	13 000	5000
16	150	1034	13 000	5000
17	150	1034	13 000	5000
18	100	689	11 000	5000
19	150	1034	13 000	5000
20	150	1034	13 000	5000
21	100	689	11 000	5000
22	150	1034	13 000	5000
23	100	689	11 000	5000

TABLE IV.- MAXIMUM ACCELERATION AND PANEL PRESSURE DATA

(a) U.S. Customary Units

[All values are full scale]

Vertical velocity, ft/sec	Horizontal velocity, ft/sec	Attitude			Normal acceleration at c.g., g units	Longitudinal acceleration at c.g., g units	Angular acceleration (pitch), rad/sec^2	Mean pressure, psi, for –												Wetted area at time of maximum acceleration, in^2	Mean pressure at time of maximum acceleration, psi
		Pitch, deg	Roll, deg	Yaw, deg				Panel A	Panel B	Panel C	Panel D	Panel E	Panel F	Panel G	Panel H	Panel I	Panel J	Panel K	Panel L		
28.72	0	-29	0	0	9.3	2.6	37.3, -23.0	43.6	[a]24.0	16.0	7.6	(b)	12.4	(b)	(b)	12.4	(b)	6.8	(b)	9 540	9.0
29.04	0	-24	0	0	11.2	3.3	45.6, -28.5	104.4	[a]32.0	10.4	(b)	(b)	23.6	(b)	(b)	23.6	(b)	7.2	(b)	9 620	10.8
29.56	0	-19	0	0	11.6	5.5	42.8, -34.2	168.4	[a]69.2	23.6	18.8	11.6	72.0	8.4	13.6	34.8	15.6	48.0	10.0	10 370	10.1
29.54	0	-15	0	0	13.4	5.0	54.5, -31.6	98.0	168.4	77.2	[a]30.0	10.8	[a]72.0	11.2	17.6	81.6	(b)	48.8	11.6	11 310	10.7
29.88	0	-13	0	0	15.2	6.0	52 , -46	103.6	164.8	71.2	37.2	12.4	[a]105.6	9.2	15.2	72.8	22.0	32.0	20.0	12 430	10.8
30.70	0	-9.5	0	0	16.0	3.7	64 , -56	[a]16.4	----	128.4	[a]36.0	38.0	104.0	27.6	35.6	----	[a]13.6	103.6	32.8	13 500	10.6
30.84	0	-9	0	0	16.1	3.6	57 , -57	[a]29.2	83.6	126.4	[a]53.6	29.6	105.6	31.2	32.8	122.4	10.8	107.2	28.0	13 500	10.8
30.98	0	-6	0	0	15.1	1.3	8.6, -34.4	[a]14.8	51.2	89.2	[a]116.0	14.5	[a]108.0	45.6	[a]19.6	105.6	18.8	62.4	14.8	15 824	8.6
31.04	0	0	0	0	15.7	0	17.2, -28.7	[a]14.4	1.3	[a]120.0	[a]144.0	45.2	[a]54.0	[a]126.8	[a]76.0	[a]40.0	16.4	42.0	36.8	18 020	8.0
30.78	0	5	0	0	15.7	0	15 , -29.9	[a]25.2	36.0	[a]88.0	104.0	112.4	11.6	131.6	116.4	101.2	20.4	14.0	106.4	16 400	8.6
30.60	0	9.5	0	0	15.3	2 , -2	35 , -26.2	[a]15.6	(b)	[a]21.2	60.0	70.8	(b)	[a]98.0	96.4	(b)	10.4	(b)	41.2	14 850	9.3
28.20	30	-29	0	0	3.4	3.4	26.7	20.0	[a]11.2	3.6	(b)	(b)	3.6	(b)	(b)	6.0	(b)	2.0	(b)	7 000	4.4
28.66	30	-25	0	0	5.8	4.0	35.4	49.6	[a]24.0	3.6	[a]7.2	(b)	10.0	(b)	(b)	13.2	5.6	3.6	(b)	10 460	5.0
29.18	30	-19	0	0	9.8	5.0	37.8	163.2	[a]71.2	30.0	[a]18.4	(b)	73.2	(b)	(b)	[a]19.2	7.6	25.2	(b)	11 330	7.8
29.68	30	-13	0	0	15.2	5.1	64.5	[a]94.4	96.8	44.2	(b)	9.2	119.2	20.8	2.3	87.2	19.2	28.8	6.8	12 880	9.2
30.52	30	-9	0	0	16.3	4.1	52.4, -11.6	[a]32.4	117.6	99.2	[a]49.2	10.8	88.4	21.6	24.0	108.8	14.0	102.8	3.3	14 260	10.4
30.60	30	-5	0	0	20.4	1.7	69.8, -14.6	[a]25.2	63.6	139.8	[a]77.2	8.8	[a]114.0	[a]40.0	[a]41.6	[a]98.8	26.8	46.8	4.8	15 950	11.6
30.60	30	6	0	0	17.8	0	51.7, -45.9	[a]20.0	33.6	[a]75.6	126.4	87.2	[a]39.6	118.0	120.8	[a]27.6	46.8	29.6	100.8	15 620	10.4
30.46	30	9	0	0	16.5	0	46 , -52	19.2	11.2	[a]45.6	84.0	100.0	34.8	[a]82.4	[a]82.0	[a]31.2	32.0	9.6	34.0	14 460	10.4
30.92	30	11	0	0	16.7	-1.7	52.7, -52.7	[a]4.0	34.4	[a]56.4	90.0	106.4	33.6	[a]98.8	[a]122.4	30.8	34.0	20.8	36.4	14 050	10.8
27.88	50	-31	0	0	3.3	5.0	17.6, -11.7	12.8	[a]8.4	(b)	(b)	(b)	2.0	(b)	(b)	17.6	(b)	(b)	(b)	6 220	4.8
27.94	50	-30	0	0	3.6	6.0	20.7	[a]22.0	[a]9.2	(b)	(b)	(b)	2.1	(b)	(b)	16.8	(b)	(b)	(b)	7 710	4.2
28.52	50	-24	0	0	4.1	4.7	34.9	20.8	[a]19.2	3.6	6.0	(b)	19.2	(b)	(b)	19.6	3.6	2.4	(b)	5 390	3.4
28.92	50	-17	0	0	7.5	5.4	46.9	110.8	[a]60.8	10.0	9.6	10.8	[a]40.4	7.6	15.6	[a]29.6	25.6	6.4	4.0	12 940	5.2
29.36	50	-14	0	0	11.2	4.7	57.8	[a]108.0	74.4	22.4	47.6	20.4	[a]101.2	18.4	23.6	59.6	18.8	16.4	4.0	13 150	7.6
30.14	50	-9	0	0	17.8	3.3	66.9	[a]42.8	125.6	87.2	[a]45.6	22.8	112.8	11.6	9.2	98.0	14.0	112.8	25.2	14 210	11.2
30.34	50	-2	0	0	25.1	3.0	93.8	[a]36.8	53.6	121.2	81.2	12.4	[a]120.8	[a]64.4	[a]94.0	[a]109.2	8.0	21.2	6.4	16 020	14.0
30.40	50	6	0	0	22.8	2.7	-41 , +73.3	18.8	23.2	[a]110.8	112.4	82.4	41.6	83.6	122.0	32.0	14.4	15.6	110.8	15 870	12.8
30.46	50	8	0	0	22.8	3.3	-53 , +59	18.0	53.6	[a]95.6	132.4	91.2	[a]39.6	105.2	111.6	[a]38.8	42.4	34.8	90.4	13 740	14.8
30.20	50	11	0	0	20.4	0	-46.9, +43.9	4.4	22.8	[a]48.0	90.8	122.4	48.8	[a]90.4	94.8	49.6	48.8	12.8	34.0	11 390	16.1
28.28	30	-31	180	0	13.2	3.9	71 , -37	44.4	[a]24.4	22.4	[a]29.6	16.0	24.0	14.4	16.8	23.6	36.4	14.4	8.8	6 880	17.2
28.86	30	-26	180	0	14.9	4.4	68.9, -48.8	73.6	[a]46.4	24.0	[a]27.2	18.0	34.0	25.6	23.6	32.8	13.6	12.0	17.6	8 190	16.3
29.36	30	-21	180	0	16.5	5.6	66 , -57.4	127.0	[a]101.0	29.2	[a]35.6	9.2	50.0	30.8	19.6	78.0	12.0	15.2	5.6	9 150	16.2
30.60	30	-15	180	0	17.8	5.6	54.5, -57.4	[a]120.0	148.4	51.2	[a]42.8	28.4	[a]105.6	19.2	24.8	[a]91.2	23.6	20.8	16.8	11 250	14.2
30.60	30	-12	180	0	17.7	5.0	66.9, -69.8	[a]56.0	106.0	123.0	[a]62.0	31.0	90.0	36.0	22.0	110.0	[a]35.0	92.0	25.0	12 540	12.7
30.84	30	-6	180	0	16.5	0	40.7, -81.5	[a]25.6	82.8	122.4	[a]109.2	12.0	[a]81.2	[a]32.0	[a]26.8	[a]88.0	16.8	86.8	22.0	15 680	9.5
30.84	30	0	180	0	14.9	0	-58.2	9.6	9.6	[a]82.0	132.8	44.8	34.0	[a]98.8	[a]107.2	[a]35.2	25.2	13.6	33.6	18 020	7.4
31.24	30	6	180	0	17.0	-2.0, +1.0	-57.8	17.6	17.2	[a]66.0	91.6	110.4	14.0	100.4	101.2	15.2	10.4	(b)	117.6	17 410	8.8
30.12	30	9	180	0	9.6	-2.6, +1.0	-63.6	(b)	11.2	[a]8.4	45.2	103.2	16.8	[a]70.8	[a]73.2	17.6	(b)	(b)	25.6	16 880	5.1
28.34	50	-33	180	0	14.1	3.4	70.8, -38.4	48.8	[a]47.2	46.8	[a]31.2	11.6	[a]36.0	24.8	23.2	27.2	31.6	25.2	11.2	5 540	22.8
28.20	50	-29	180	0	14.6	3.0	73.3, -49.8	59.6	[a]47.6	34.8	[a]22.8	14.4	[a]30.0	24.8	31.2	[a]26.4	39.6	16.4	7.2	6 670	19.6
29.18	50	-23	180	0	16.2	4.5	64.9, -64.9	117.6	[a]76.0	36.4	[a]45.6	12.8	[a]42.8	32.8	27.6	[a]43.6	22.4	22.0	7.6	8 240	17.7
29.76	50	-18	180	0	18.7	5.8	52.4, -72.8	126.0	[a]109.6	24.8	[a]31.6	20.4	[a]61.6	44.4	22.8	[a]70.0	32.0	12.4	14.4	9 340	18.0
29.50	50	-17	180	0	16.6	5.7	52.7, -73.3	137.6	[a]80.4	32.4	[a]30.8	17.6	[a]104.8	52.0	24.8	[a]73.2	11.6	12.0	11.6	9 150	16.4
30.34	50	-13	180	0	18.0	5.5	44.3, -85.6	94.8	152.8	113.6	[a]17.2	25.2	[a]108.8	36.8	26.8	[a]132.0	[a]13.2	42.4	14.0	10 850	14.9
30.52	50	-10	180	0	18.7	3.8	50.1, -94.4	[a]29.6	106.0	131.6	[a]73.2	27.6	116.0	28.8	40.8	115.6	26.4	100.0	23.6	13 070	12.9
32.00	50	-5	180	0	17.3	-2.0	17.7, -82.6	12.4	15.2	99.6	[a]105.2	32.8	[a]70.8	97.6	105.2	[a]67.6	34.4	31.2	56.6	15 890	9.8
30.34	50	0	180	0	15.9	-2.1	-50.2	(b)	8.0	[a]74.8	100.4	51.6	[a]52.4	[a]126.8	[a]125.2	42.4	30.4	6.0	24.0	18 020	8.0
29.88	50	9	180	0	9.5	-3.7	-70.3	8.4	18.8	17.6	54.0	195.2	12.0	84.4	102.8	12.4	4.8	32.0	57.2	14 140	6.0

[a]Integrated panel pressure.

[b]Value too low to read.

TABLE IV.- MAXIMUM ACCELERATION AND PANEL PRESSURE DATA – Concluded

(b) International System of Units (SI)

[All values are full scale]

Vertical velocity, m/sec	Horizontal velocity, m/sec	Attitude			Normal acceleration at c.g., g units	Longitudinal acceleration at c.g., g units	Angular acceleration (pitch), rad/sec^2	Mean pressure, psi, for –												Wetted area at time of maximum acceleration, m^2	Mean pressure at time of maximum acceleration, kN/m^2
		Pitch, deg	Roll, deg	Yaw, deg				Panel A	Panel B	Panel C	Panel D	Panel E	Panel F	Panel G	Panel H	Panel I	Panel J	Panel K	Panel L		
8.75	0	-29	0	0	9.3	2.6	37.3, -23.0	301	[a]165	110	52	(b)	85	(b)	(b)	85	(b)	47	(b)	6.15	62
8.85	0	-24	0	0	11.2	3.3	45.6, -28.5	720	[a]220	72	(b)	(b)	163	(b)	(b)	163	(b)	50	(b)	6.21	74
9.01	0	-19	0	0	11.6	5.5	42.8, -34.2	1161	[a]477	163	130	80	496	58	94	240	108	331	69	6.69	70
9.00	0	-15	0	0	13.4	5.0	54.5, -31.6	676	1161	532	[a]207	74	[a]496	77	121	563	(b)	336	80	7.30	74
9.11	0	-13	0	0	15.2	6.0	52 , -46	714	1136	491	256	85	[a]728	63	105	502	152	221	138	8.02	74
9.36	0	-9.5	0	0	16.0	3.7	64 , -56	[a]113	----	885	[a]248	262	717	190	245	---	[a]94	714	226	8.71	73
9.40	0	-9	0	0	16.1	3.6	57 , -57	[a]201	576	871	[a]370	204	728	215	226	844	74	739	193	8.71	74
9.44	0	-6	0	0	15.1	1.3	8.6, -34.4	[a]102	353	615	[a]800	100	[a]745	314	[a]135	728	130	430	102	10.21	59
9.46	0	0	0	0	15.7	0	17.2, -28.7	[a]99	9	[a]827	[a]993	312	[a]372	[a]874	[a]524	[a]276	113	290	254	11.63	55
9.38	0	5	0	0	15.7	0	15 , -29.9	[a]174	248	[a]607	717	775	80	907	803	698	141	97	734	10.58	59
9.33	0	9.5	0	0	15.3	2, , -2	35 , -26.2	[a]108	(b)	[a]146	414	488	(b)	[a]676	665	(b)	72	(b)	284	9.58	64
8.60	9.1	-29	0	0	3.4	3.4	26.7	138	[a]77	25	(b)	(b)	25	(b)	(b)	41	(b)	14	(b)	4.52	30
8.74	9.1	-25	0	0	5.8	4.0	35.4	342	[a]165	25	[a]50	(b)	69	(b)	(b)	91	39	25	(b)	6.75	34
8.89	9.1	-19	0	0	9.8	5.0	37.8	1125	[a]491	207	[a]127	(b)	505	(b)	(b)	[a]132	52	174	(b)	7.31	54
9.05	9.1	-13	0	0	15.2	5.1	64.5	[a]651	667	305	(b)	63	822	143	16	601	132	199	47	8.31	63
9.30	9.1	-9	0	0	16.3	4.1	52.4, -11.6	[a]223	811	684	[a]339	74	609	149	165	750	97	709	23	9.20	72
9.33	9.1	-5	0	0	20.4	1.7	69.8, -14.6	[a]174	439	964	[a]532	61	[a]786	[a]276	[a]287	[a]681	185	323	33	10.29	80
9.33	9.1	6	0	0	17.8	0	51.7, -45.9	[a]138	232	[a]521	871	601	[a]273	814	833	[a]190	323	204	695	10.08	72
9.28	9.1	9	0	0	16.5	0	46 , -52	132	77	[a]314	579	689	240	[a]568	[a]565	[a]215	221	66	234	9.33	72
9.42	9.1	11	0	0	16.7	-1.7	52.7, -52.7	[a]28	237	[a]389	621	734	232	[a]681	[a]844	212	234	143	251	9.06	74
8.50	15.0	-31	0	0	3.3	5.0	17.6, -11.7	88	[a]58	(b)	(b)	(b)	14	(b)	(b)	121	(b)	(b)	(b)	4.01	33
8.52	15.0	-30	0	0	3.6	6.0	20.7	[a]151	[a]63	(b)	(b)	(b)	14	(b)	(b)	116	(b)	(b)	(b)	4.97	29
8.69	15.0	-24	0	0	4.1	4.7	34.9	143	[a]132	25	41	(b)	132	(b)	(b)	135	25	17	(b)	3.48	23
8.81	15.0	-17	0	0	7.5	5.4	46.9	764	[a]419	69	66	74	[a]279	52	108	[a]204	177	44	28	8.35	36
8.95	15.0	-14	0	0	11.2	4.7	57.8	[a]745	513	154	328	141	[a]698	127	163	411	130	113	28	8.48	52
9.19	15.0	-9	0	0	17.8	3.3	66.9	[a]295	866	601	[a]314	157	778	80	634	676	97	778	174	9.17	77
9.25	15.0	-2	0	0	25.1	3.0	93.8	[a]254	370	836	560	85	[a]833	[a]444	[a]648	[a]753	55	146	44	10.34	97
9.27	15.0	6	0	0	22.8	2.7	-41 , +73.3	130	160	[a]764	775	568	287	576	841	221	99	108	764	10.24	88
9.28	15.0	8	0	0	22.8	3.3	-53 , + 59	124	370	[a]659	913	629	[a]273	725	769	[a]268	292	240	623	8.86	102
9.20	15.0	11	0	0	20.4	0	-46.9, +43.9	30	157	[a]331	626	844	336	[a]623	654	342	336	88	234	7.35	111
8.62	9.1	-31	180	0	13.2	3.9	71 , -37	306	[a]168	154	[a]204	110	165	99	116	163	251	99	61	4.44	119
8.80	9.1	-26	180	0	14.9	4.4	68.9, -48.8	507	[a]320	165	[a]188	124	234	177	163	226	94	83	121	5.28	112
8.95	9.1	-21	180	0	16.5	5.6	66 , -57.4	876	[a]696	201	[a]245	63	345	212	135	538	83	105	39	5.90	112
9.33	9.1	-15	180	0	17.8	5.6	54.5, -57.4	[a]827	1023	353	[a]295	196	[a]728	132	171	[a]629	163	143	116	7.26	98
9.33	9.1	-12	180	0	17.7	5.0	66.9, -69.8	[a]386	731	848	[a]427	214	621	248	152	758	[a]241	634	172	8.09	88
9.40	9.1	-6	180	0	16.5	0	40.7, -81.5	[a]177	571	844	[a]753	83	[a]560	[a]221	[a]185	[a]607	116	598	152	10.12	66
9.40	9.1	0	180	0	14.9	0	-58.2	66	66	[a]565	916	309	234	[a]681	[a]739	[a]243	174	94	232	11.63	51
9.52	9.1	6	180	0	17.0	-2.0, +1.0	-57.8	121	119	[a]455	632	761	97	692	698	105	72	(b)	811	11.23	61
9.18	9.1	9	180	0	9.6	-2.6, +1.0	-63.6	(b)	77	[a]58	312	712	116	[a]488	[a]504	121	(b)	(b)	177	10.89	35
8.64	15.0	-33	180	0	14.1	3.4	70.8, -38.4	336	[a]325	323	[a]215	80	[a]248	171	160	188	218	174	77	3.57	157
8.60	15.0	-29	180	0	14.6	3.0	73.3, -49.8	411	[a]328	240	[a]157	99	[a]207	171	215	[a]182	273	113	50	4.30	135
8.89	15.0	-23	180	0	16.2	4.5	64.9, -64.9	811	[a]524	251	[a]314	88	[a]295	226	190	[a]301	154	152	52	5.32	122
9.07	15.0	-18	180	0	18.7	5.8	52.4, -72.8	869	[a]756	171	[a]218	141	[a]425	306	157	[a]483	221	85	99	6.03	124
8.99	15.0	-17	180	0	16.6	5.7	52.7, -73.3	949	[a]554	223	[a]212	121	[a]723	359	171	[a]505	80	83	80	5.90	113
9.25	15.0	-13	180	0	18.0	5.5	44.3, -85.6	654	1054	783	[a]119	173	[a]750	254	185	[a]910	[a]91	292	97	7.00	103
9.30	15.0	-10	180	0	18.7	3.8	50.1, -94.4	[a]204	731	907	[a]505	190	800	199	281	797	182	689	163	8.39	89
9.75	15.0	-5	180	0	17.3	-2.0	17.7, -82.6	85	105	687	[a]725	226	[a]488	673	725	[a]466	237	215	390	10.25	68
9.25	15.0	0	180	0	15.9	-2.1	-50.2	(b)	55	[a]516	692	356	[a]361	[a]874	[a]863	292	210	41	165	11.63	55
9.11	15.0	9	180	0	9.5	-3.7	-70.3	58	130	121	372	1346	83	582	709	85	33	221	394	9.12	41

[a]Integrated panel pressure.

[b]Value too low to read.

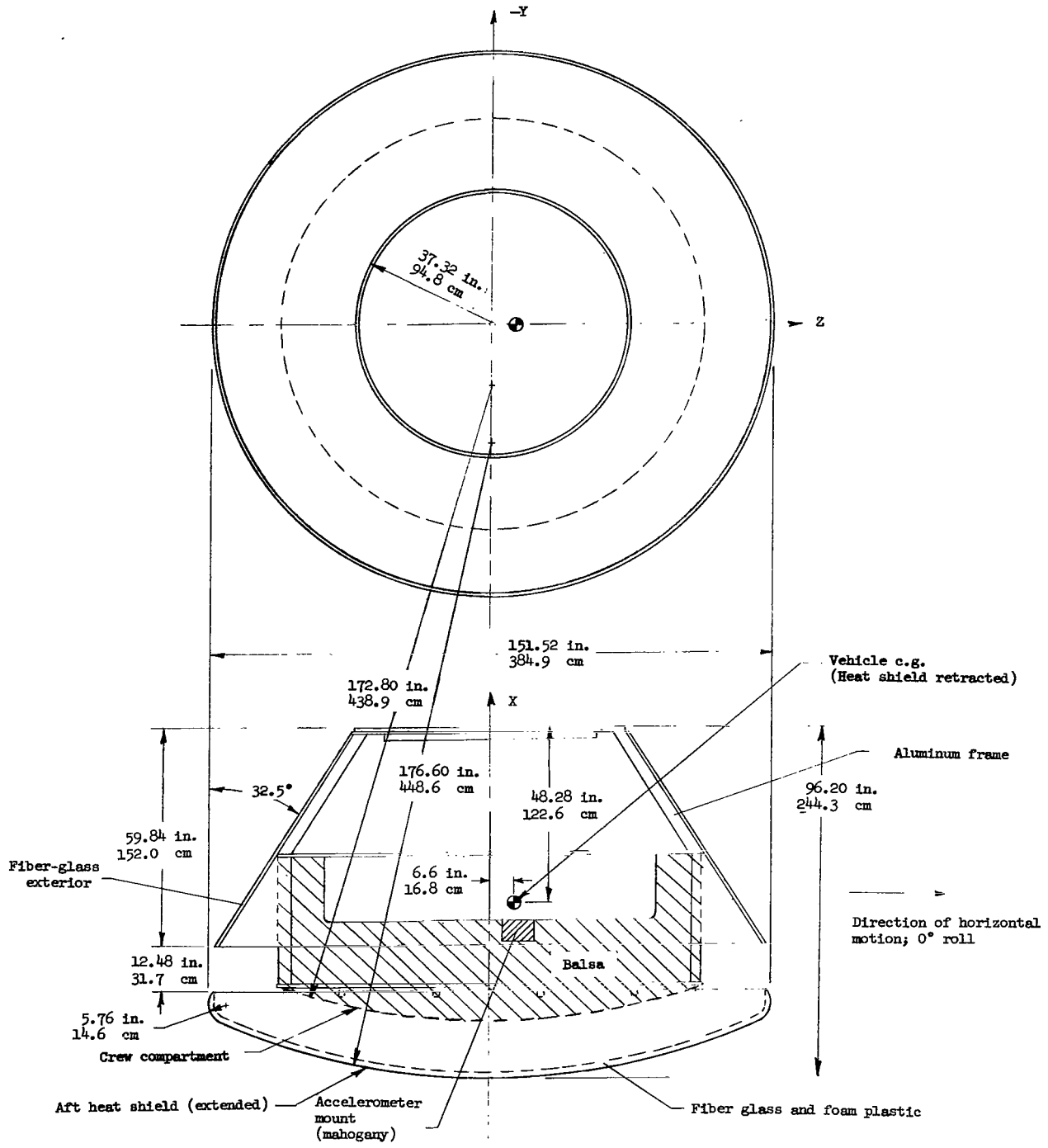

Figure 1.- General arrangement of 1/4-scale dynamic model. All values are full scale.

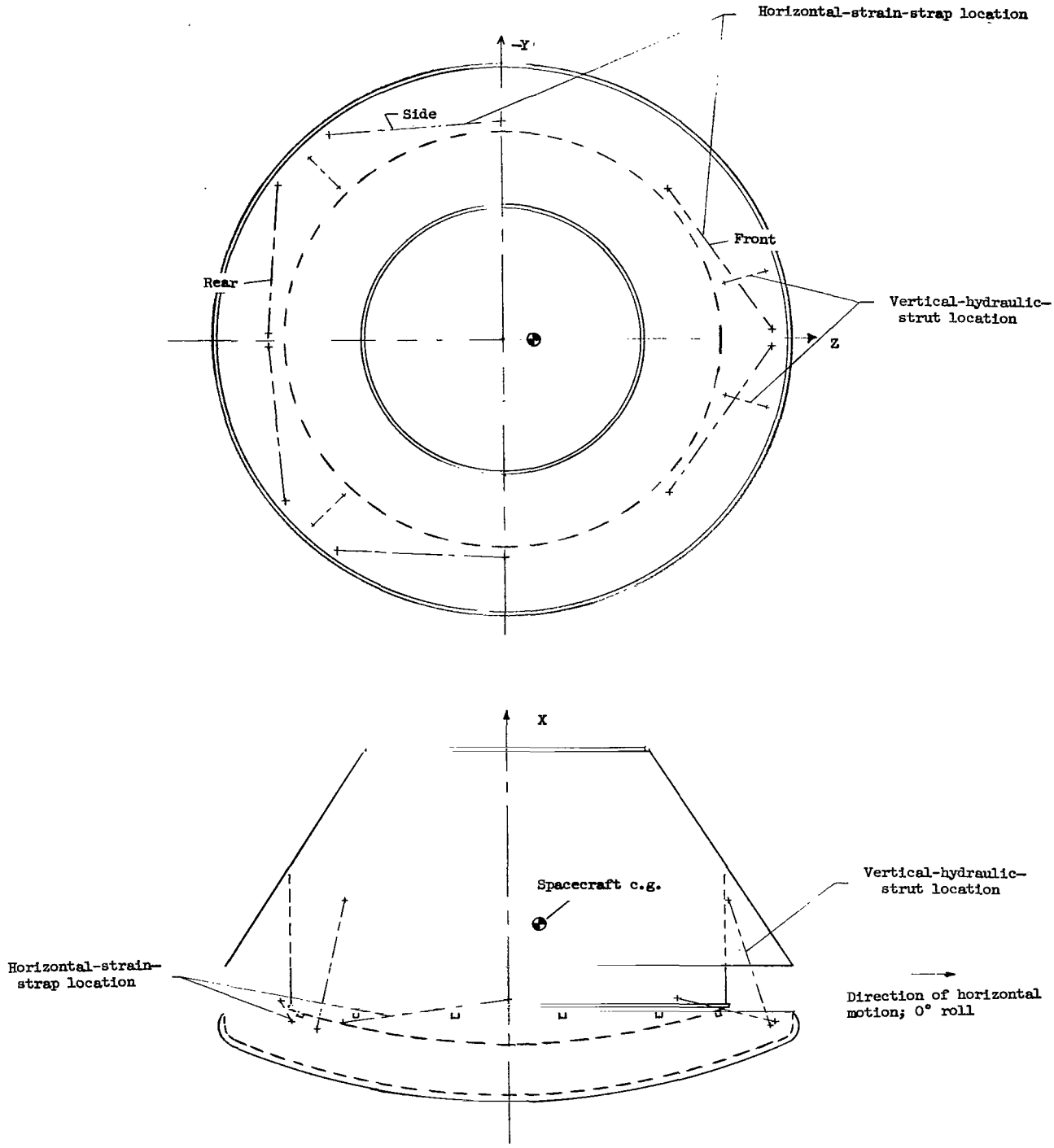

Figure 2.- Location of the landing-gear components.

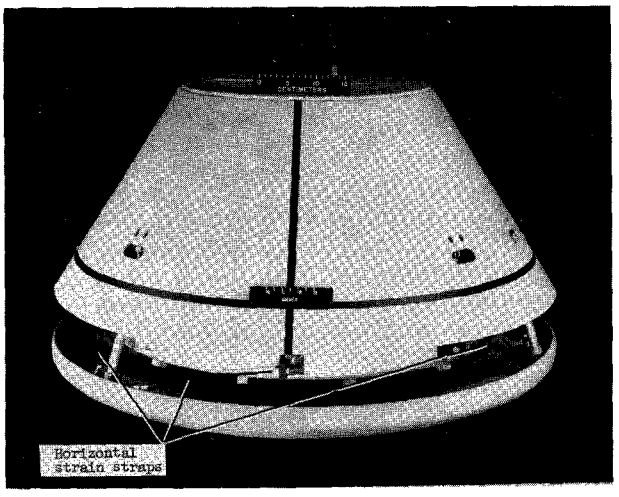

Side view L-64-5269

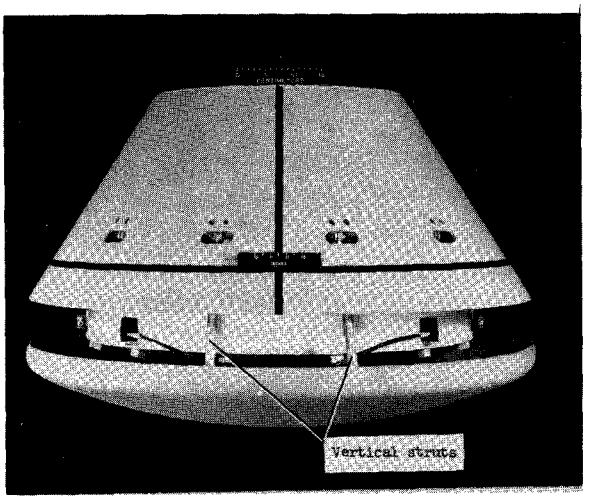

Front view L-64-5270

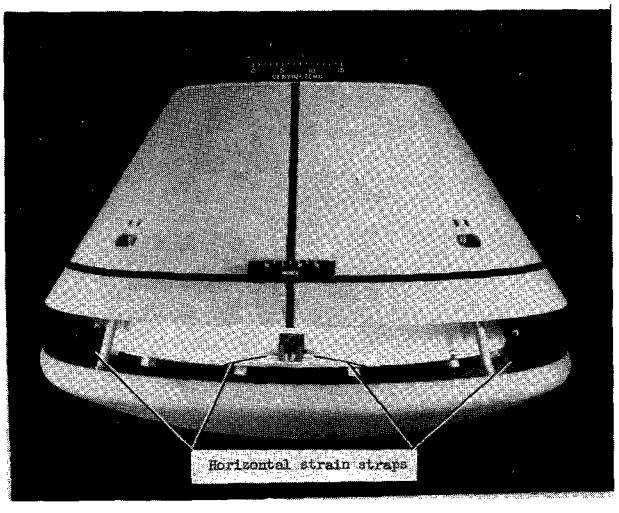

Rear view L-64-5273

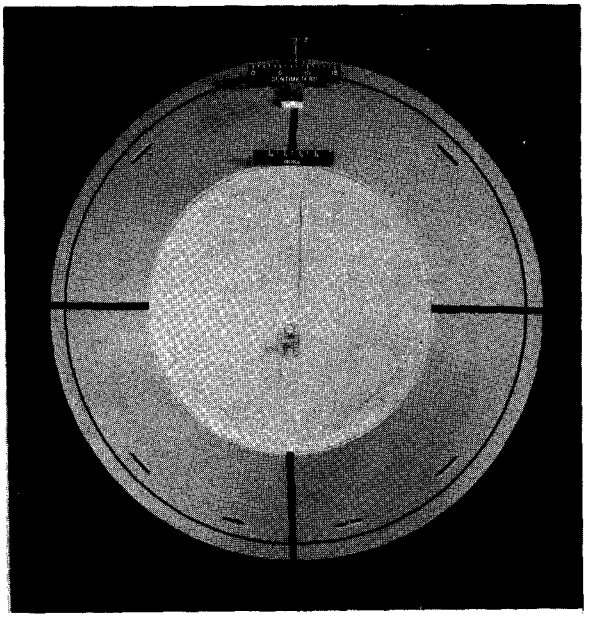

Top view L-64-5272

Figure 3.- Photographs of 1/4-scale model.

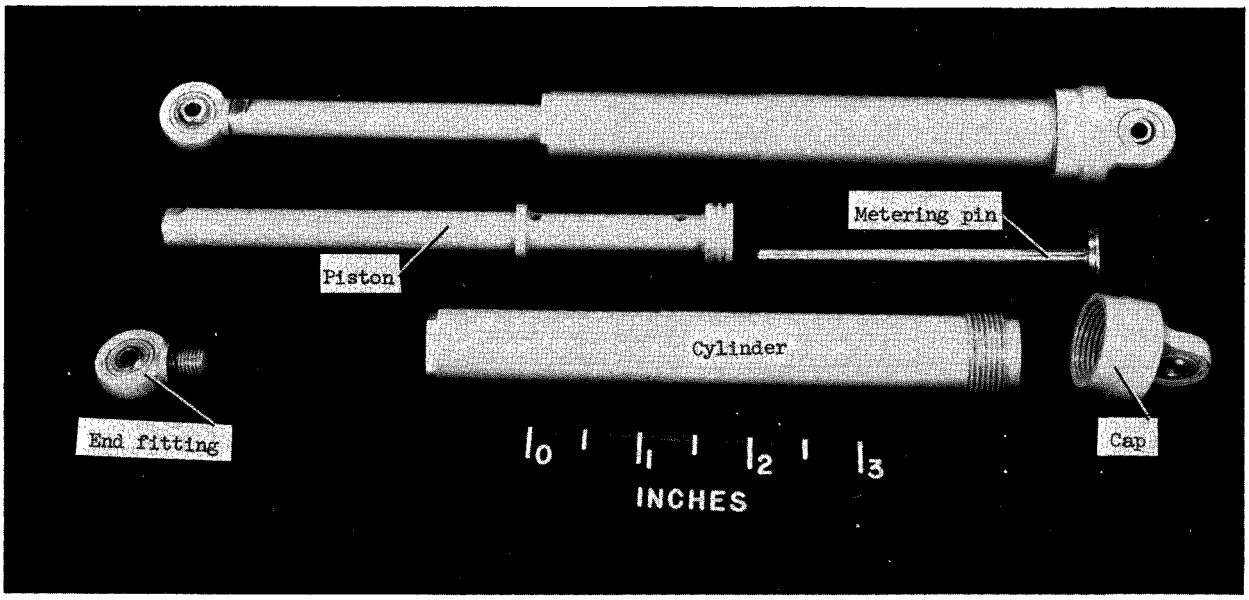

(a) Vertical hydraulic strut. L-63-6189.1

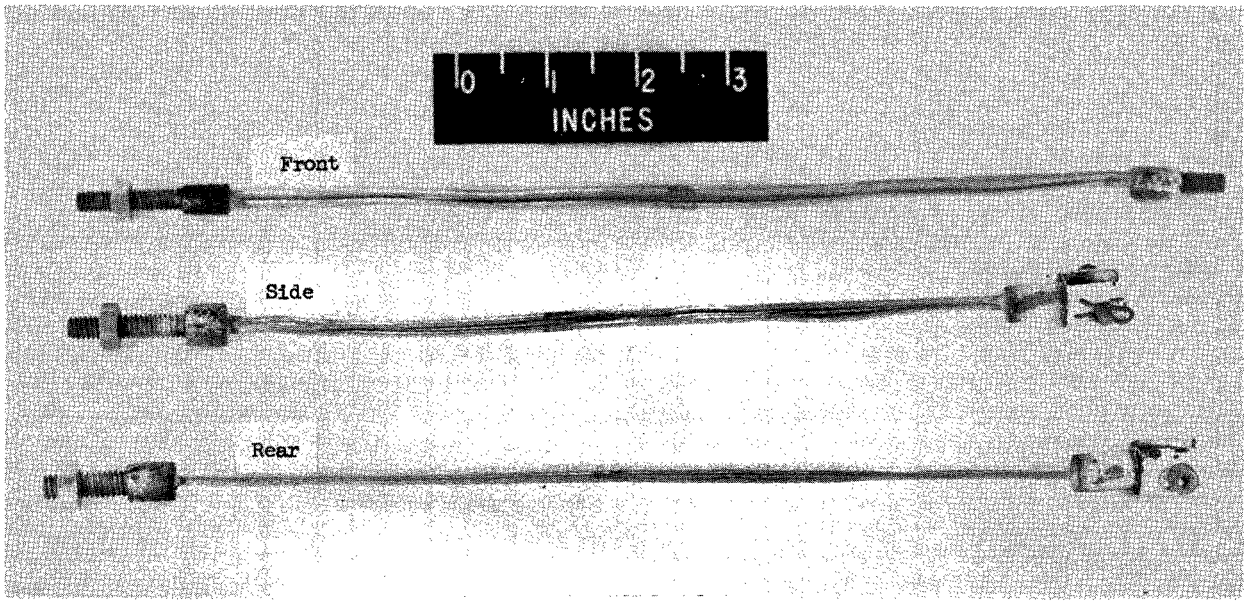

(b) Horizontal strain straps. L-65-6109.1

Figure 4.- Landing-system elements.

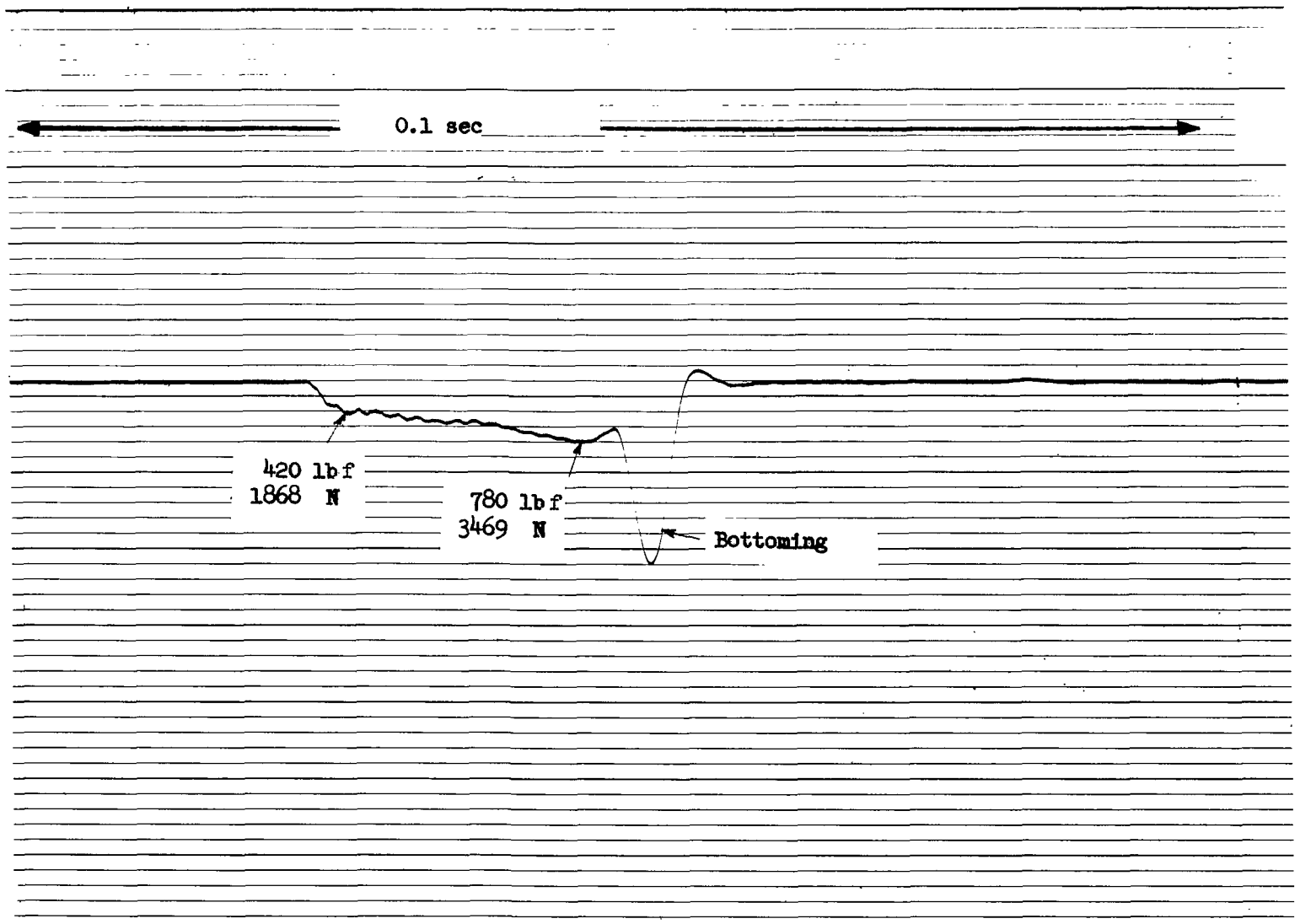

Figure 5.- Force characteristics for vertical hydraulic strut. All values are model scale. Impacting mass, 1.24 slugs (18.1 kg); velocity at impact, 15 ft/sec (4.6 m/sec).

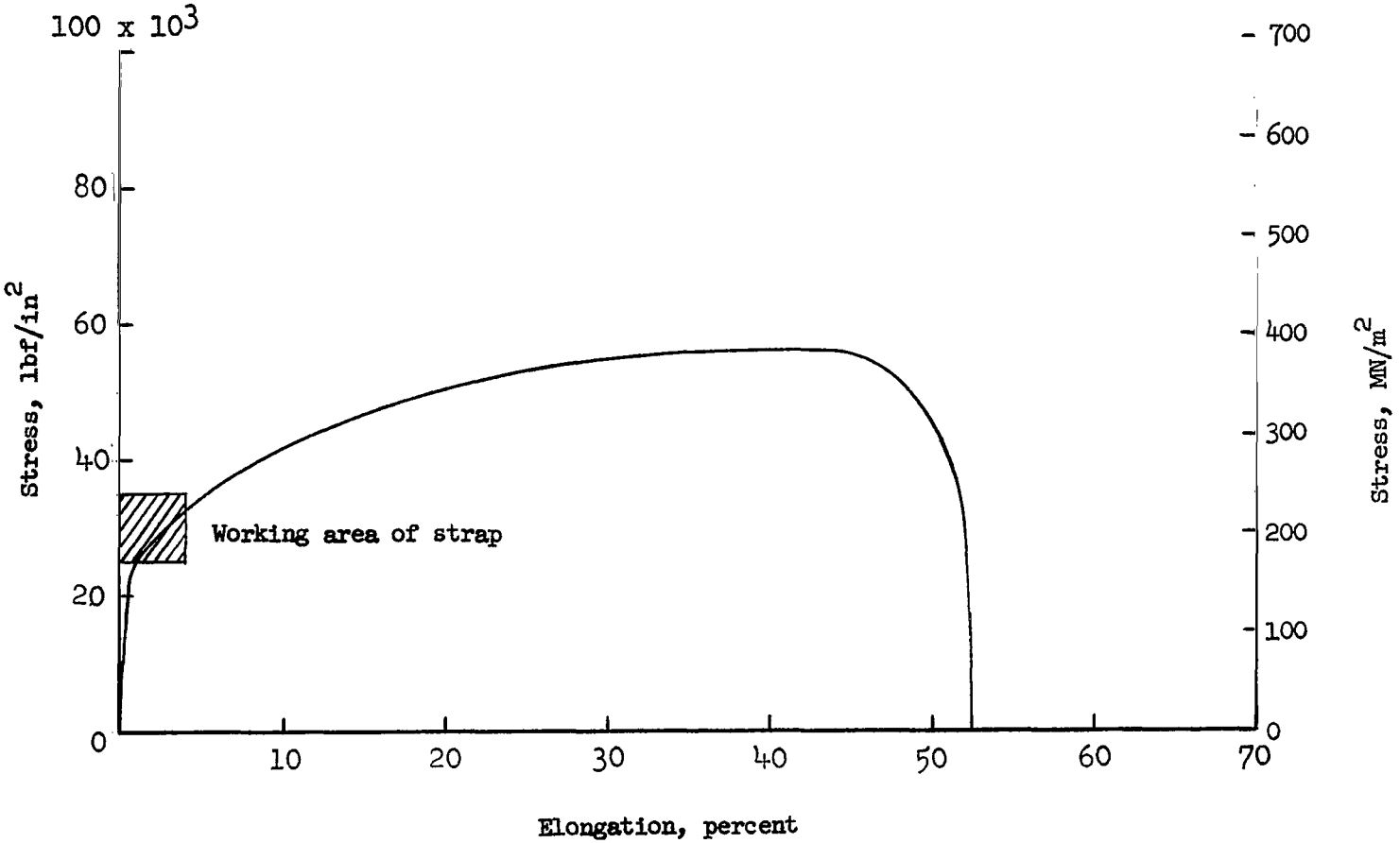

Figure 6.- Stress-strain characteristics of low-carbon nickel wire used as horizontal strain straps.

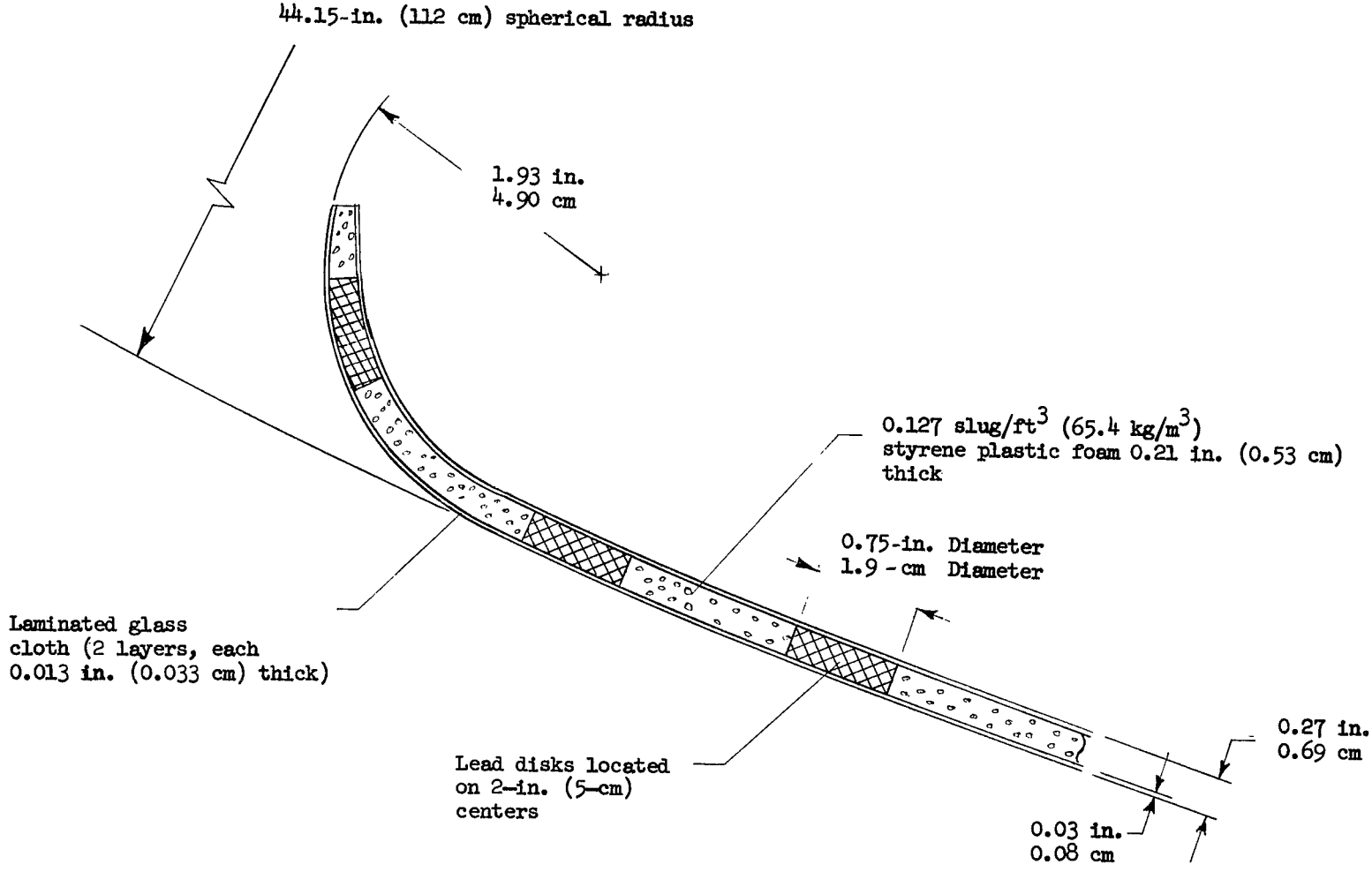

Figure 7.- Heat-shield construction details (model values).

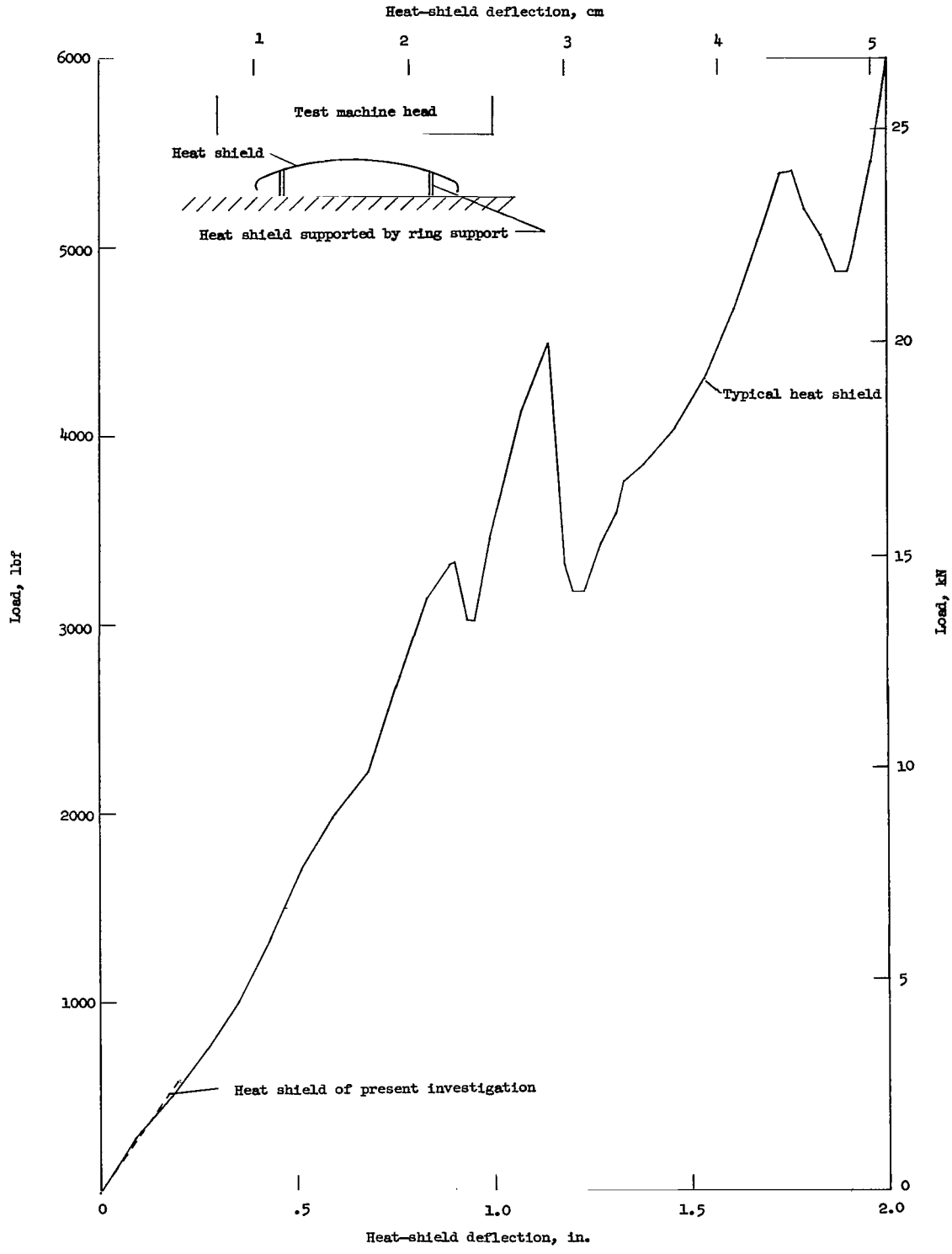

Figure 8.- Load-deflection characteristics for heat shield. All values are model scale.

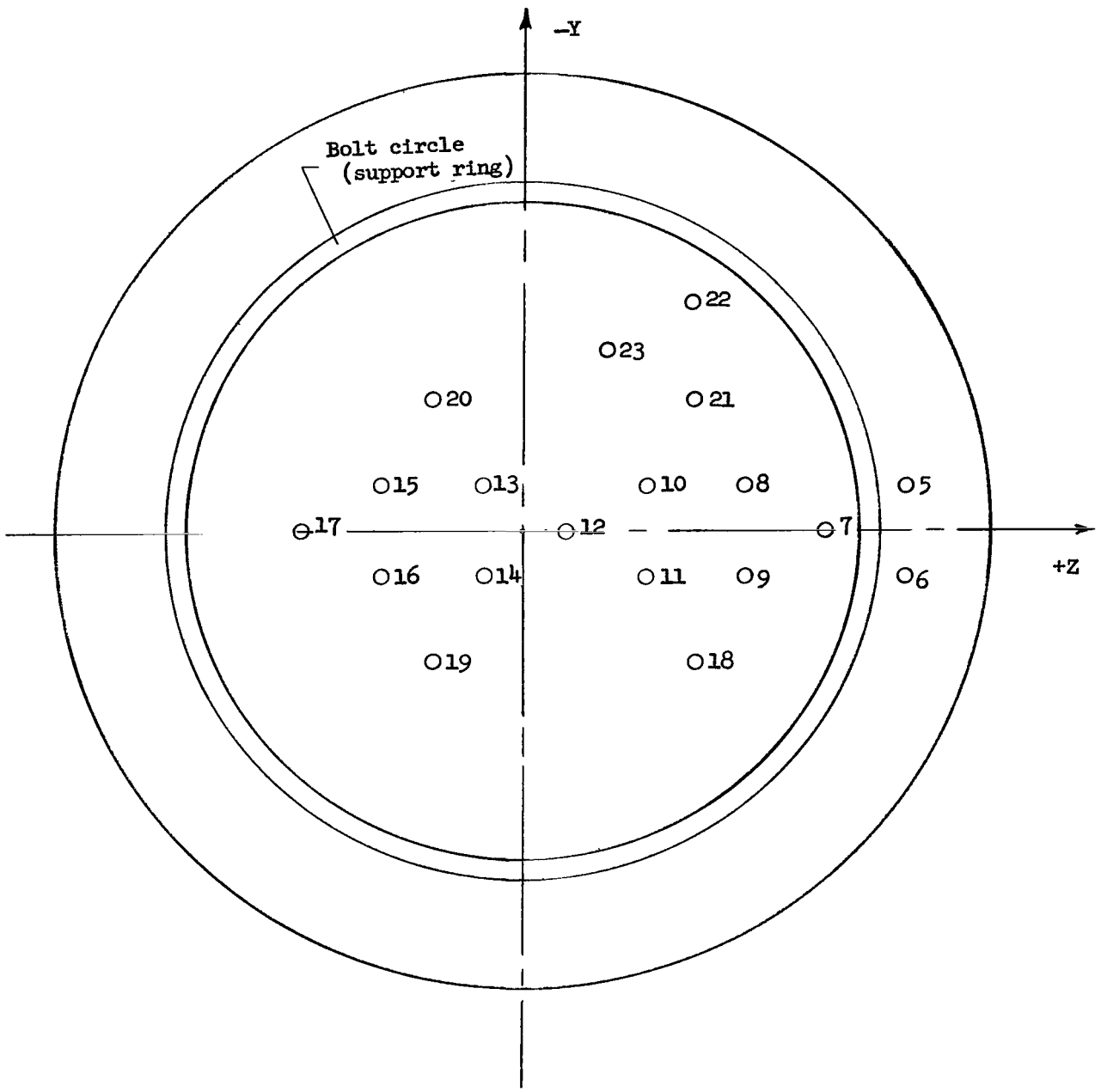

Figure 9.- Pressure-gage locations on inside of aft heat shield. Model diameter, 37.88 in. (96.2 cm). Numbers 5 to 23 are arbitrarily assigned to the pressure transducers.

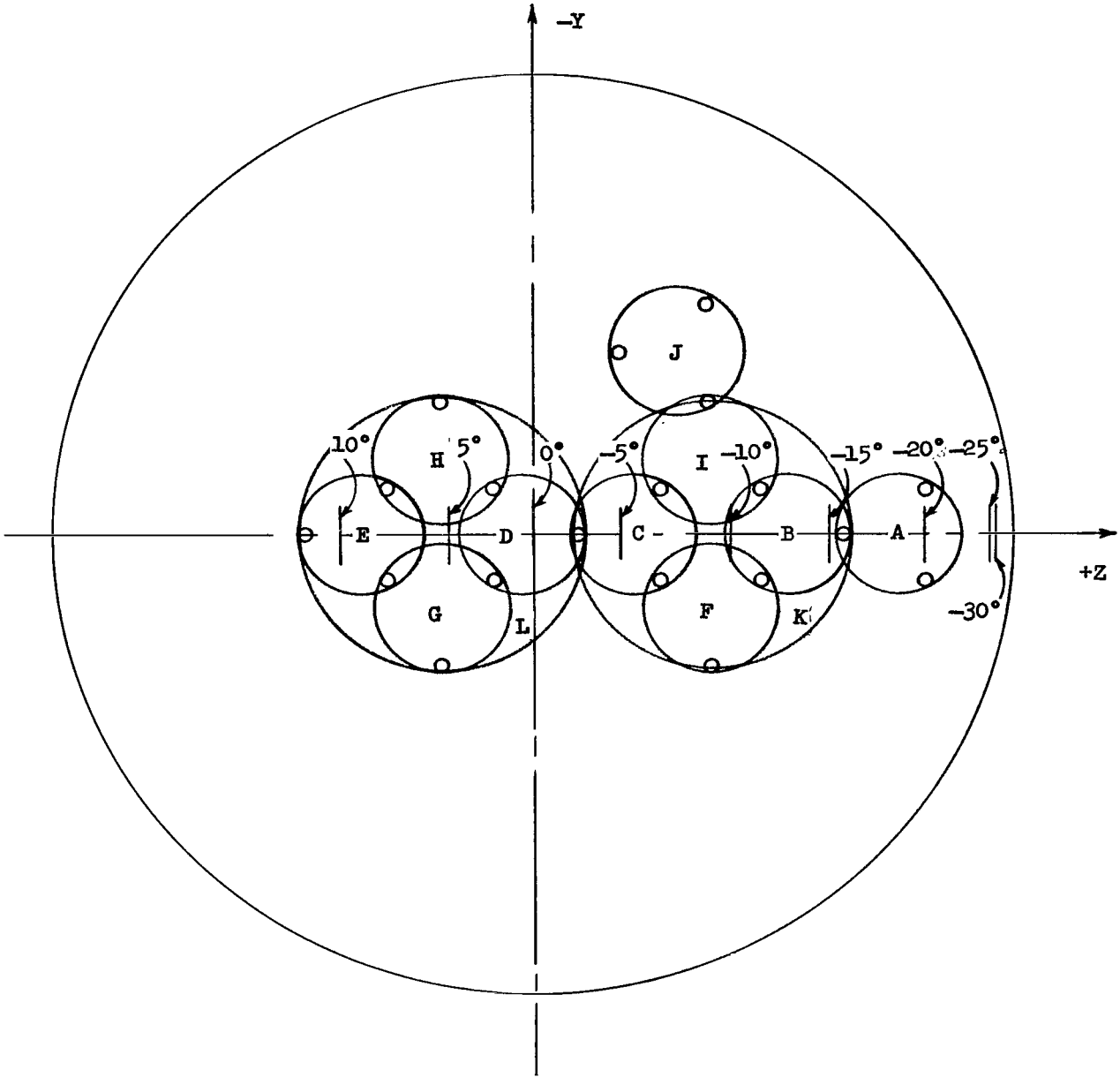

Figure 10.- Arbitrary panel areas and initial impact-attitude locations. Panels A, B, C, D, and E each represent a full-scale area of 1.6 ft^2 (0.15 m^2); panels F, G, H, I, and J each represent a full-scale area of 1.9 ft^2 (0.18 m^2); panels K and L each represent a full-scale area of 10.9 ft^2 (1.01 m^2). Tick marks on Z-axis show initial points of water contact on the heat shield for various pitch attitudes.

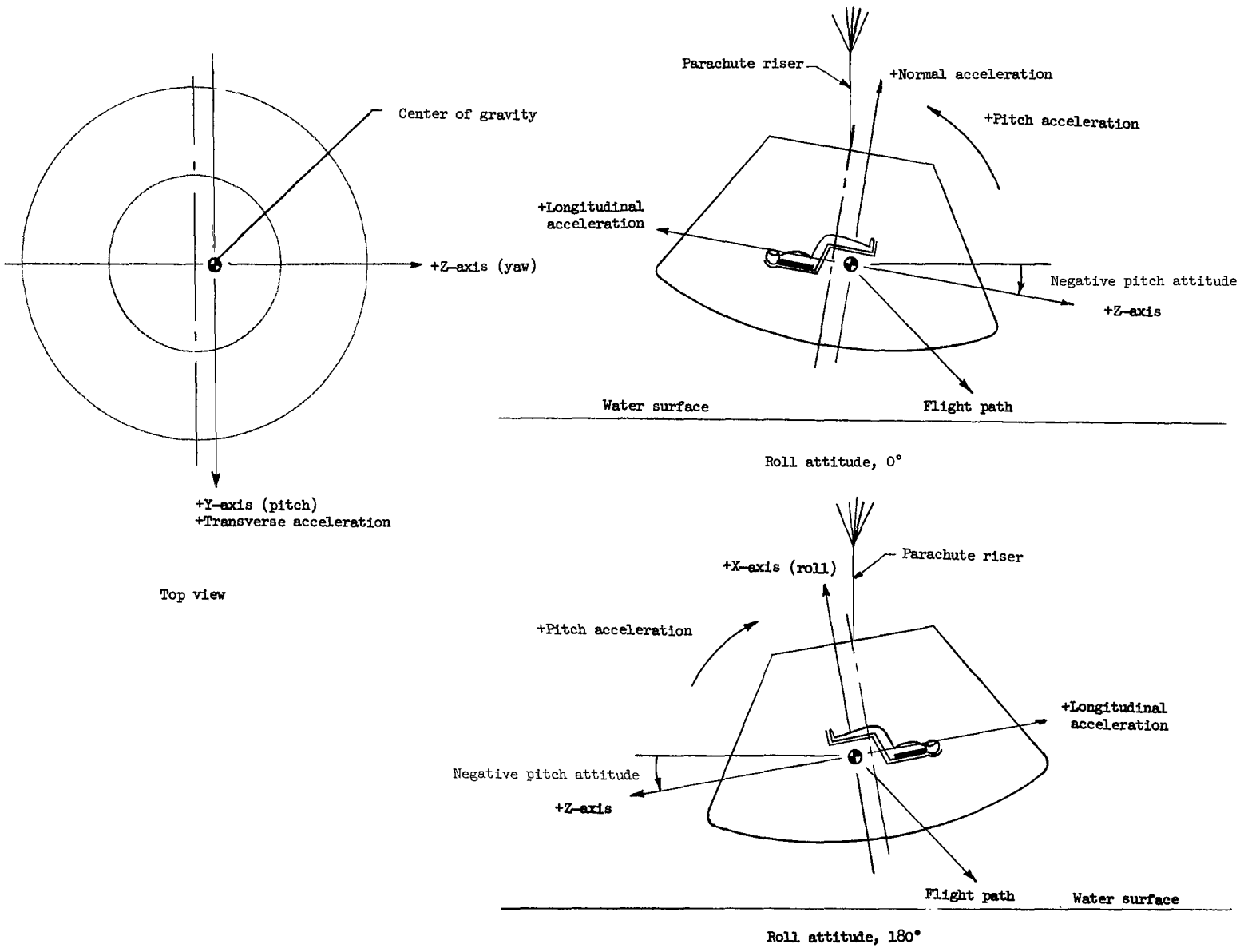

Figure 11.- Acceleration axes, attitudes, force directions, and flight path.

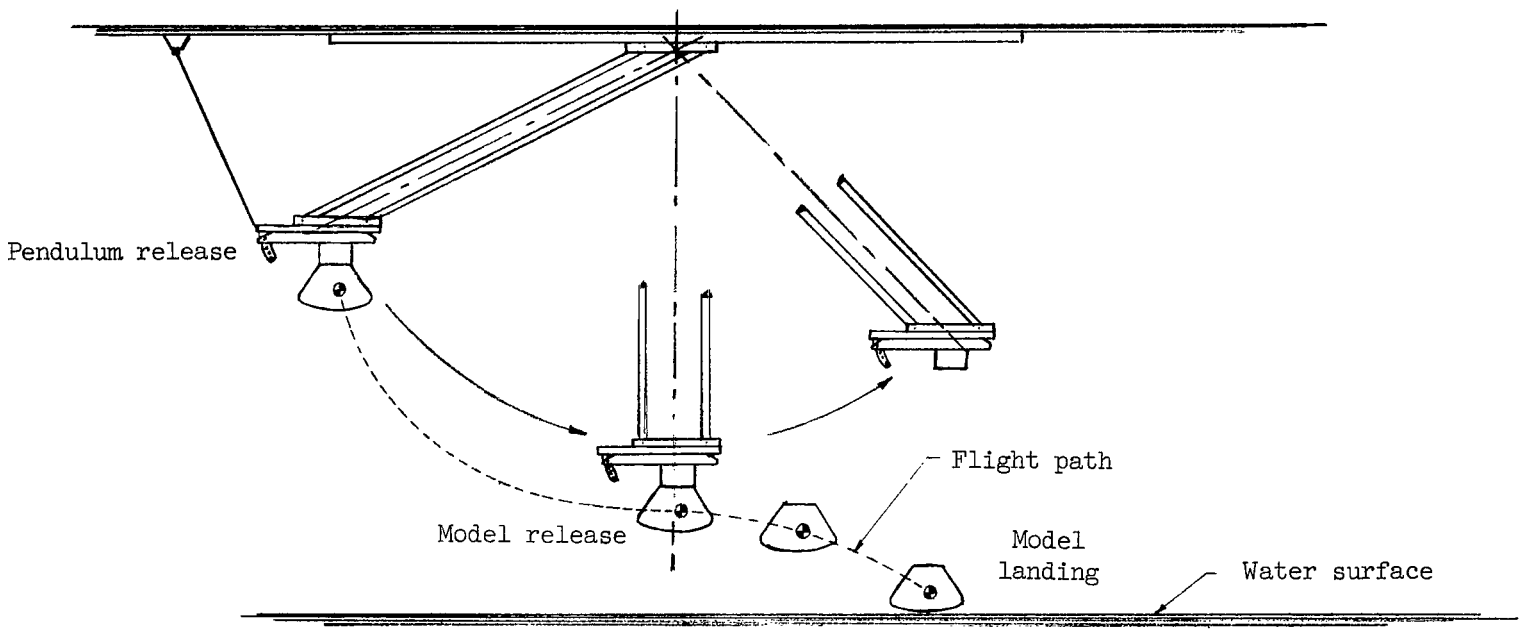

Figure 12.- Pendulum operation during typical model launch and landing.

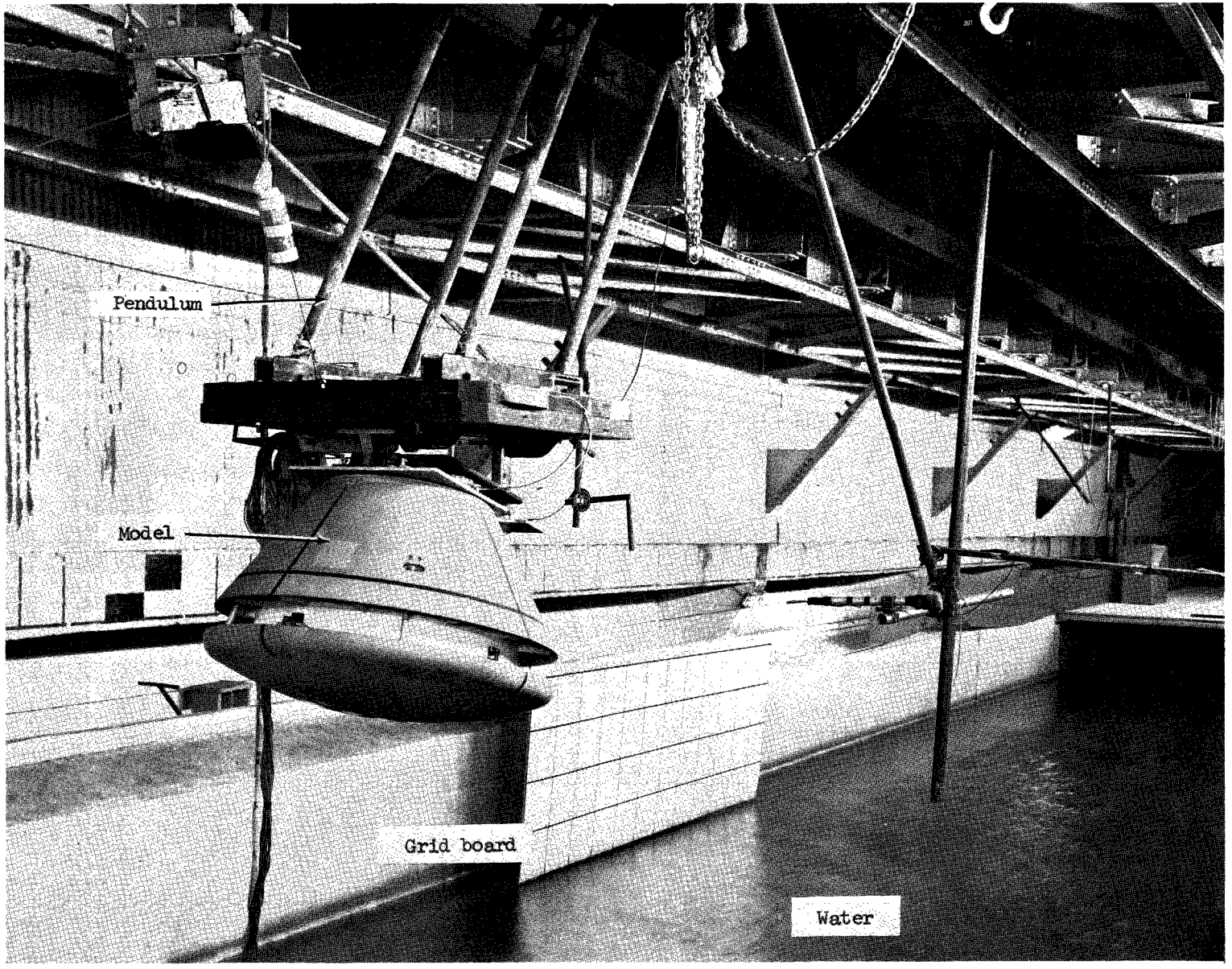

Figure 13.- Test-area setup showing model on carriage in pulled-back position.

L-65-3650.1

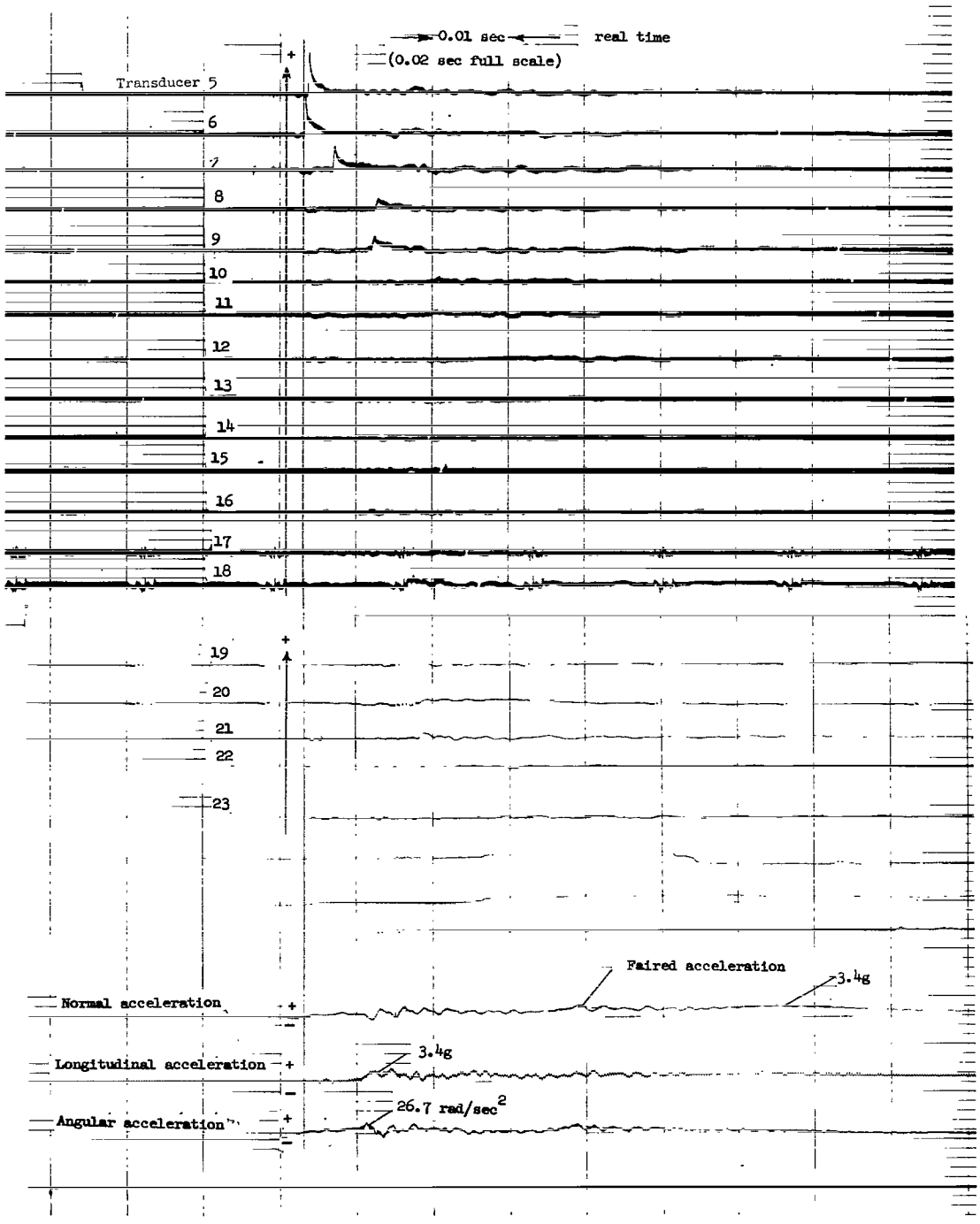

(a) Pitch attitude, -29°.

Figure 14.- Typical oscillograph records of accelerations and pressures. Vertical velocity, approximately 30 ft/sec (9.1 m/sec); horizontal velocity, 30 ft/sec (9.1 m/sec); roll, 0°; yaw, 0°. All values are full scale unless otherwise indicated.

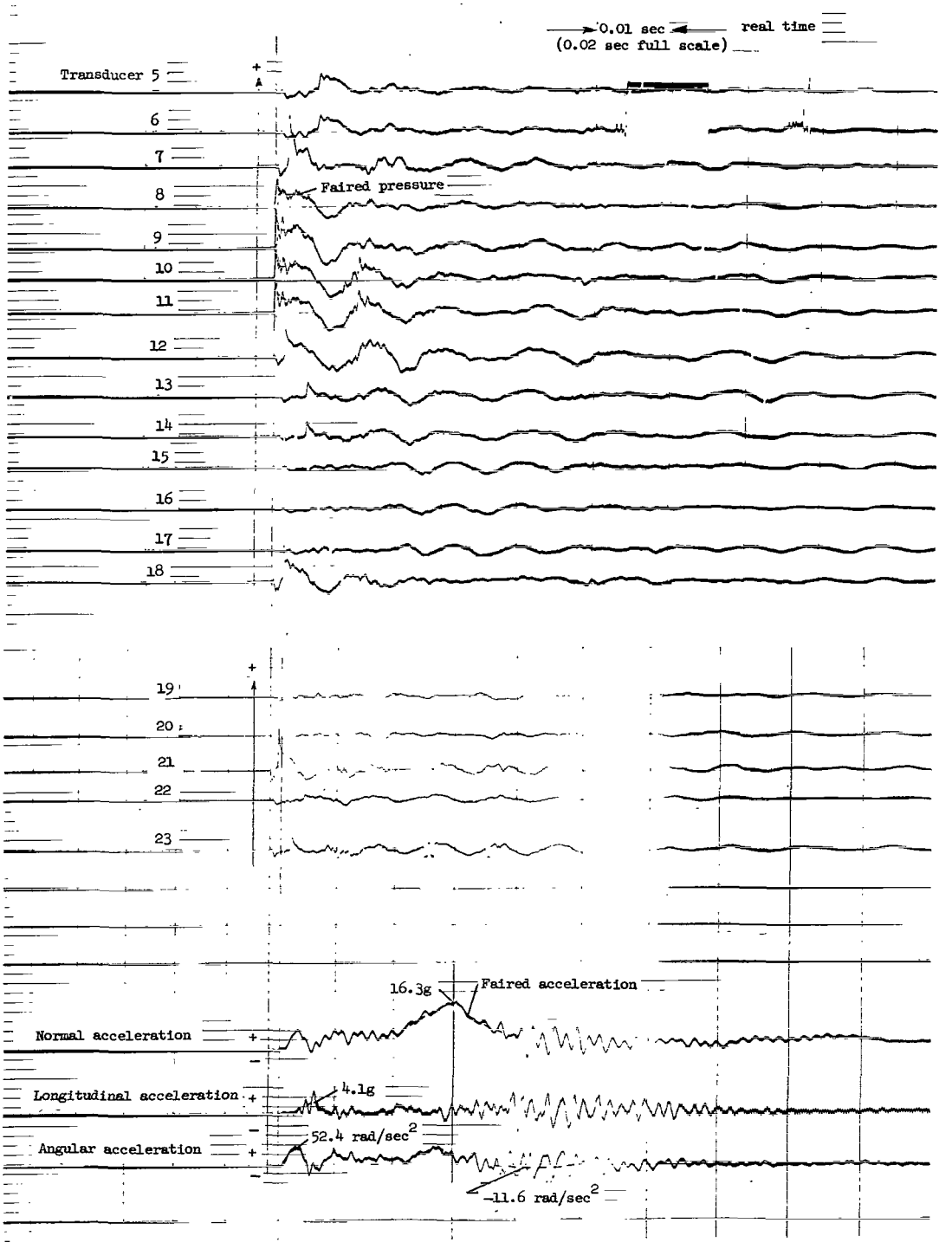

(b) Pitch attitude, -9°.

Figure 14.- Continued.

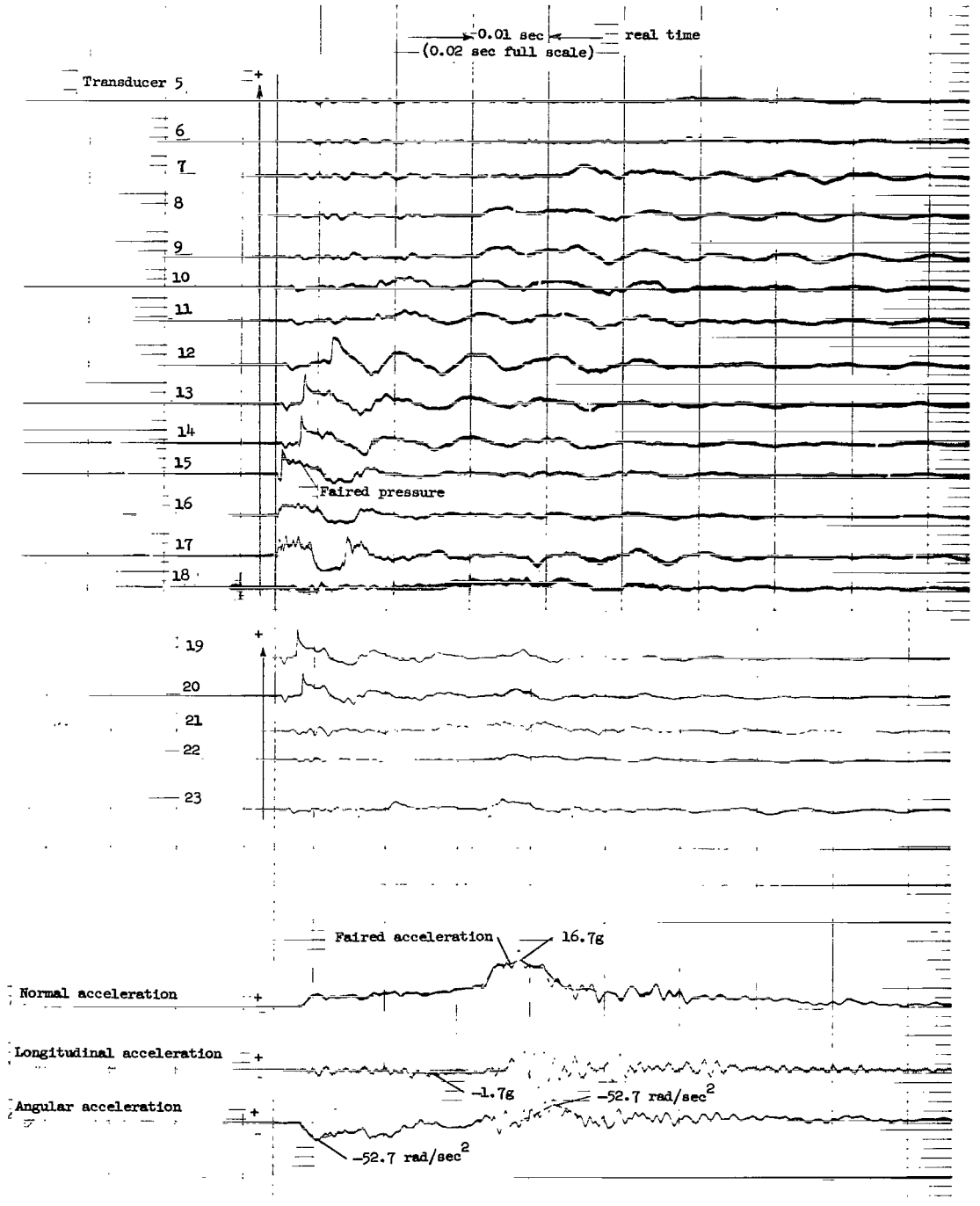

(c) Pitch attitude, 11°.

Figure 14.- Concluded.

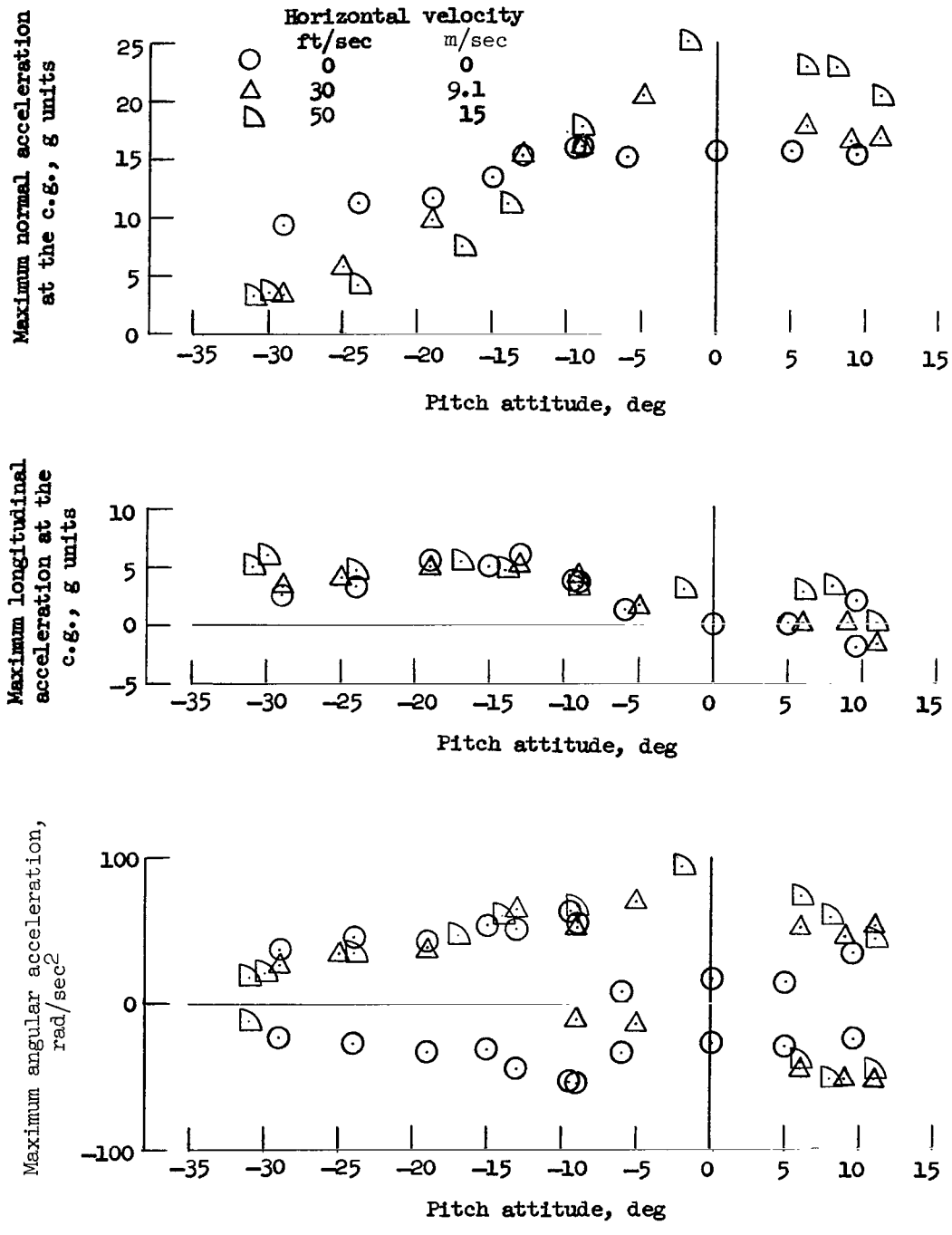

(a) Roll attitude, 0^{o}.

Figure 15.- Maximum acceleration data. Vertical velocity, 30 ft/sec (9.1 m/sec). All values are full scale.

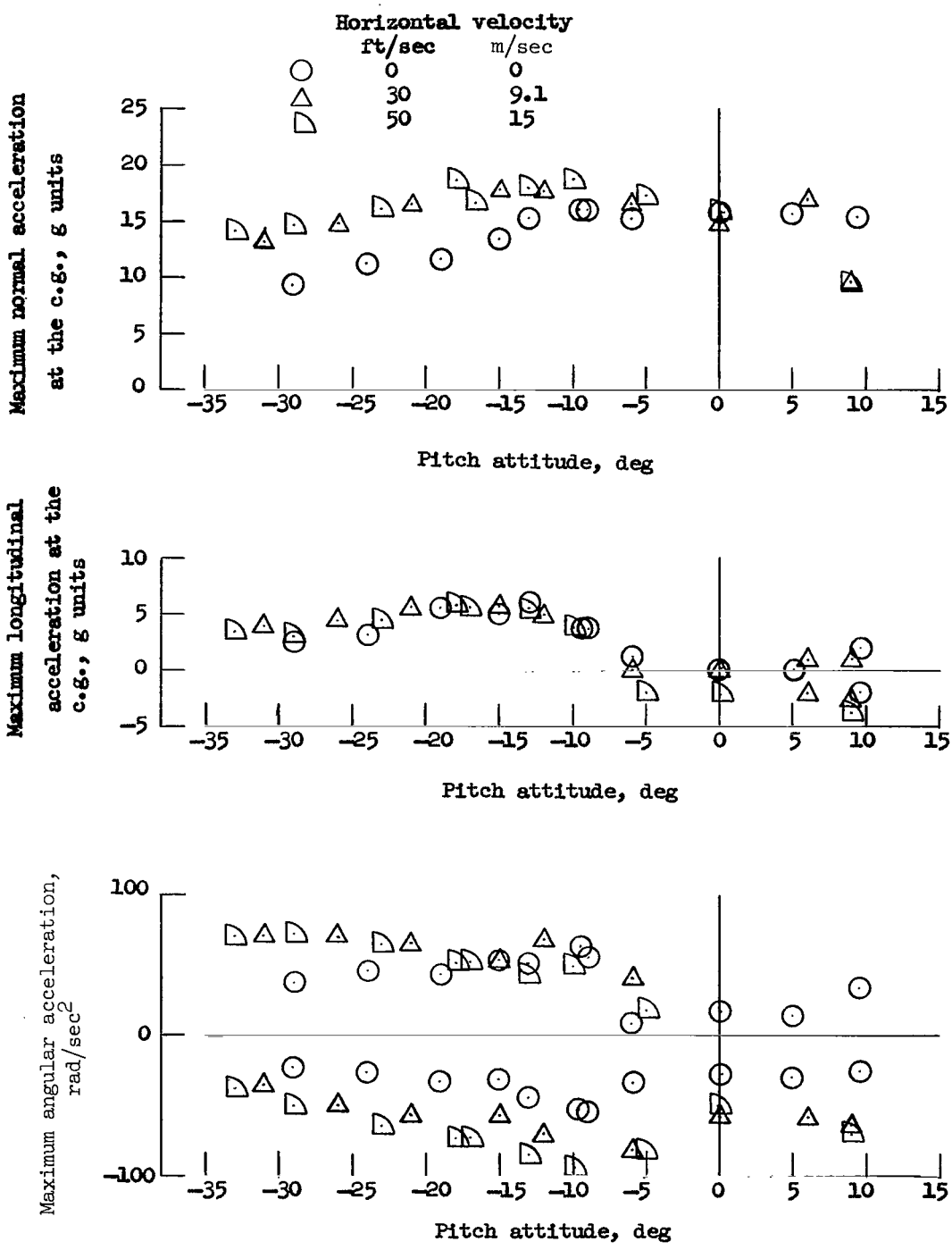

(b) Roll attitude, 180°.

Figure 15.- Concluded.

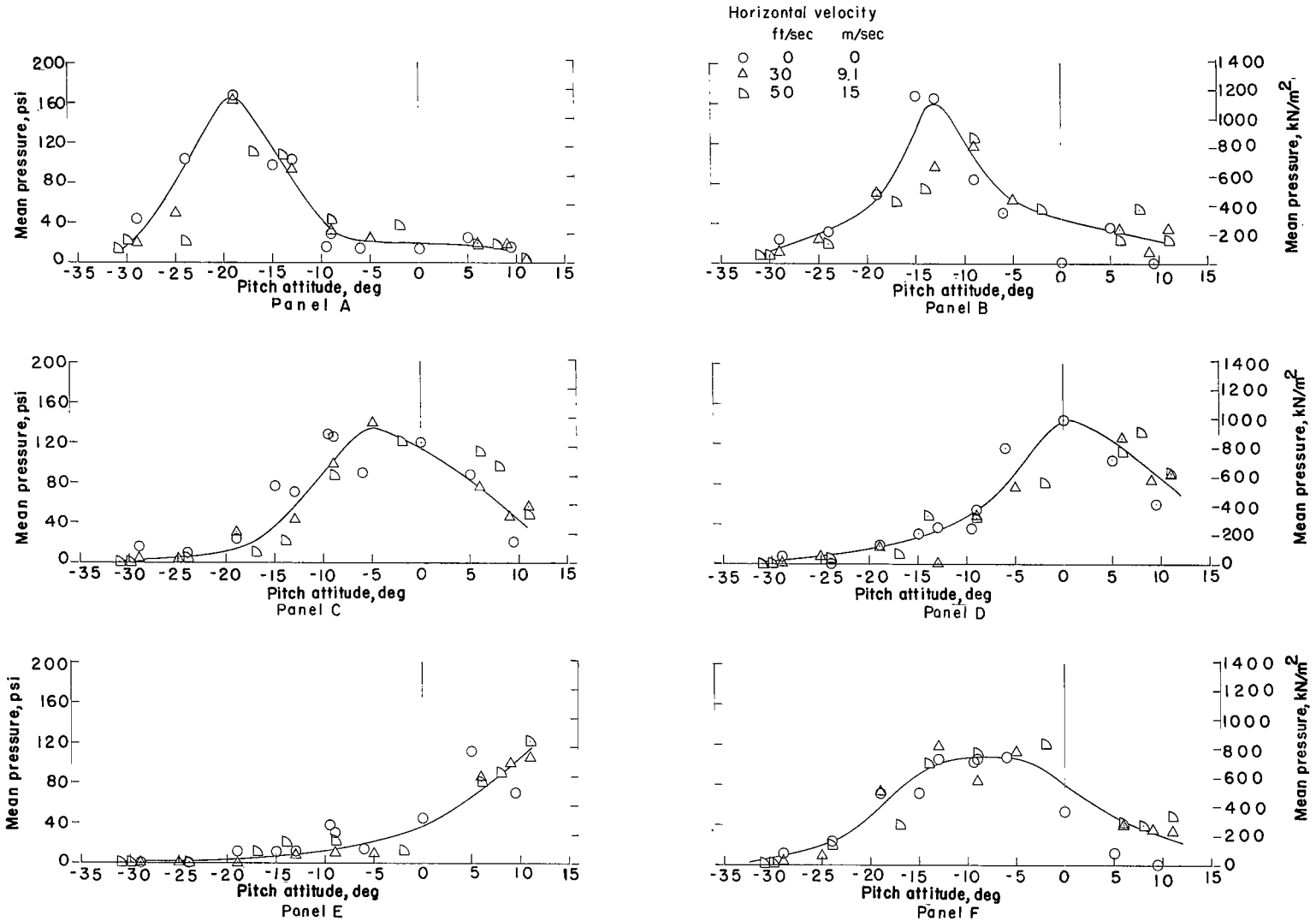

(a) Panels A to F.

Figure 16.- Panel-pressure data for vehicle at 0^0 roll. Vertical velocity, 28 to 31 ft/sec (8.5 to 9.4 m/sec); yaw, 0^0. All values are full scale.

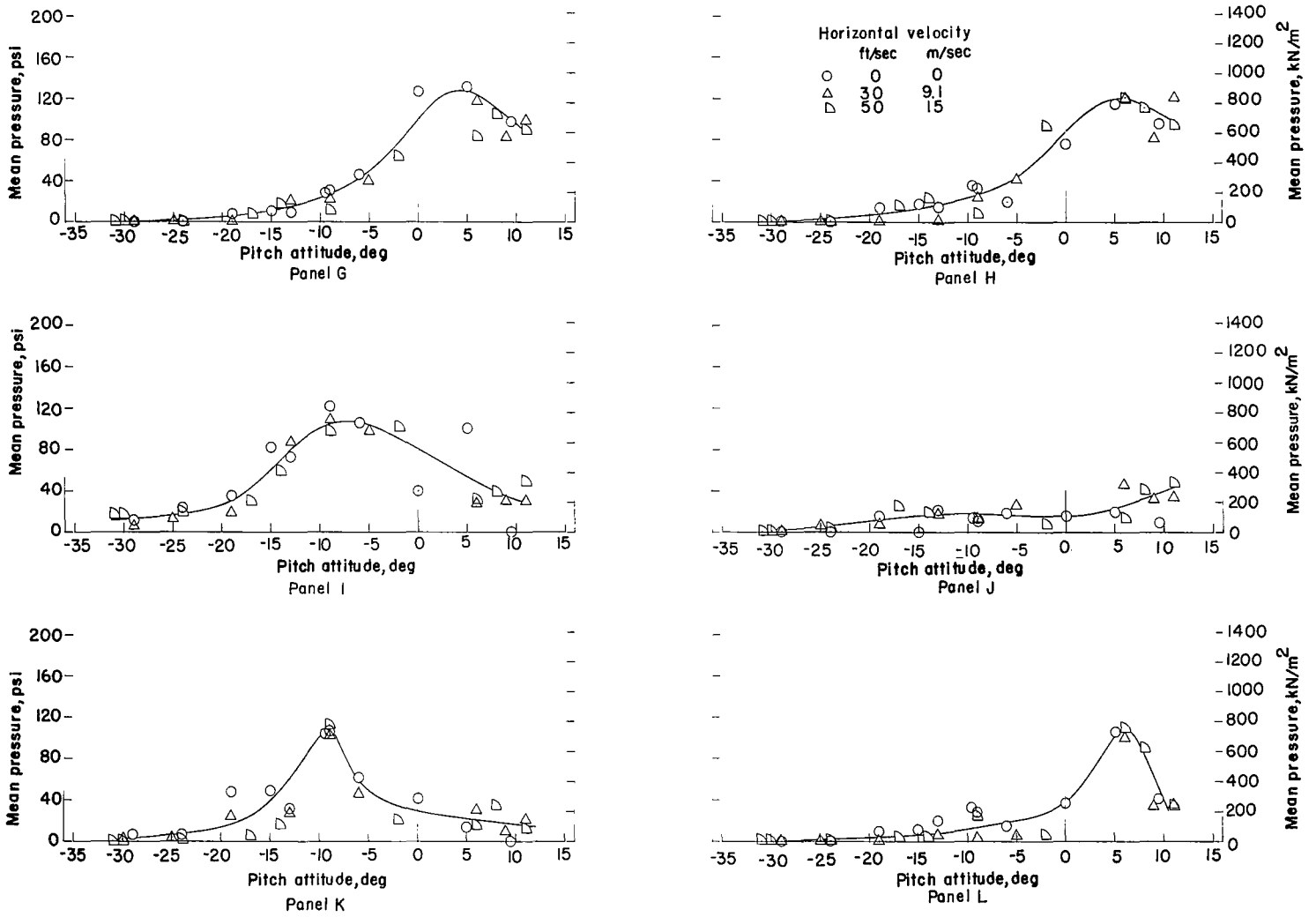

(b) Panels G to L.

Figure 16.- Concluded.

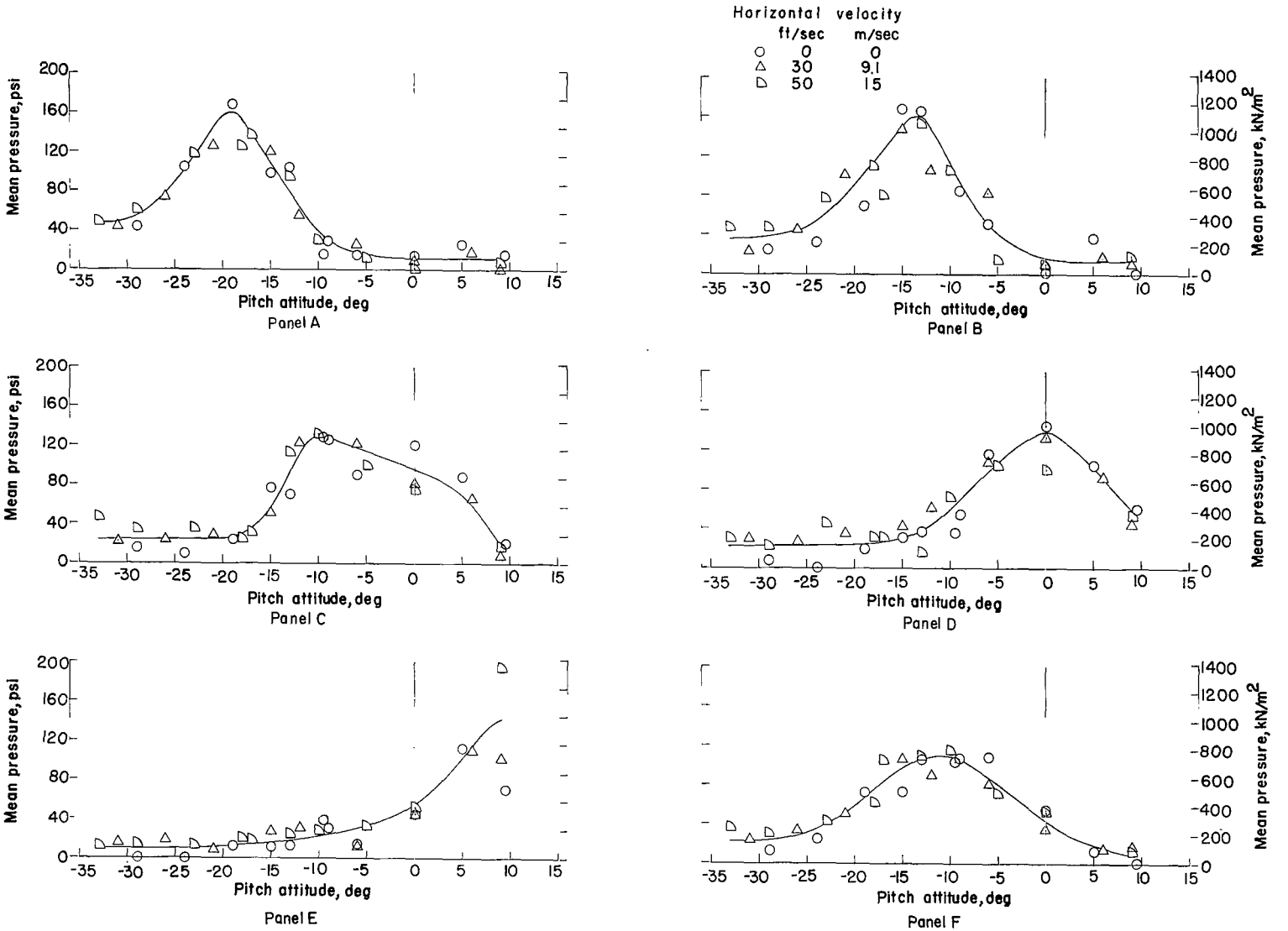

(a) Panels A to F.

Figure 17.- Panel-pressure data for vehicle at 180° roll. Vertical velocity, 28 to 31 ft/sec (8.5 to 9.4 m/sec); yaw, 0°. All values are full scale.

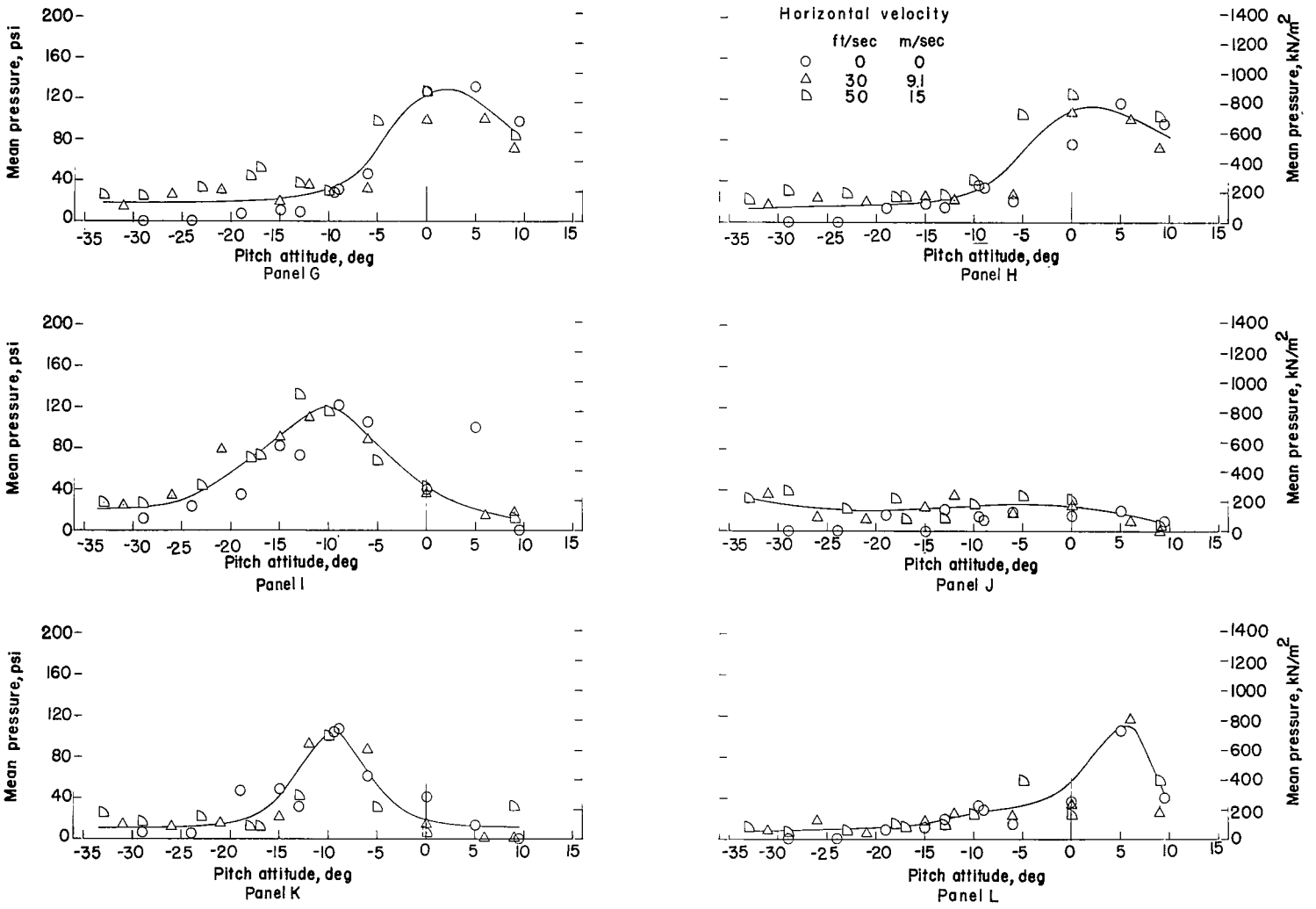

(b) Panels G to L.

Figure 17.- Concluded.

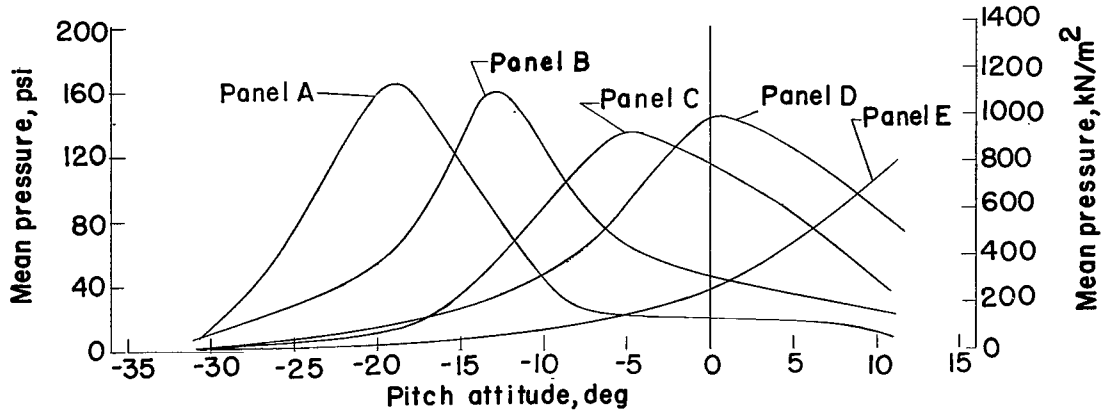

(a) Panels with area of 1.6 ft^2 (0.15 m^2).

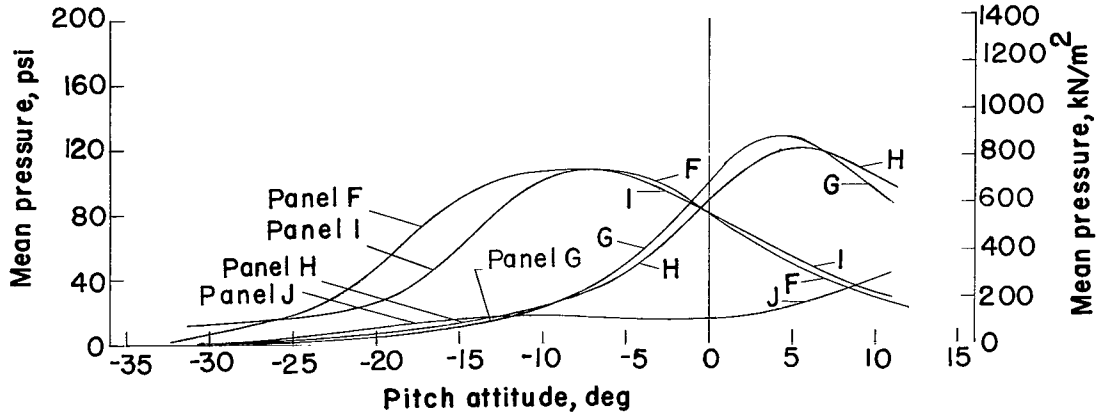

(b) Panels with area of 1.9 ft^2 (0.18 m^2).

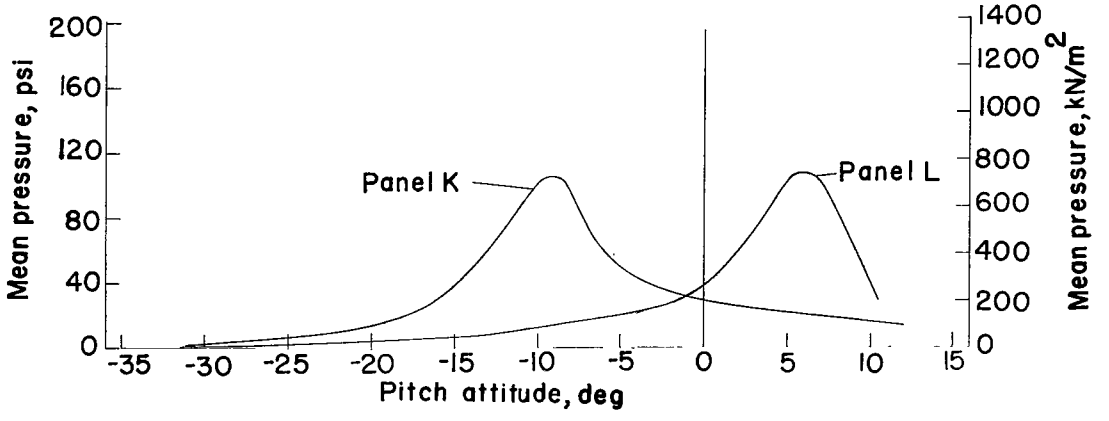

(c) Panels with area of 10.9 ft^2 (1.01 m^2).

Figure 18.- Fairings of panel-pressure data for vehicle at 0^0 roll. Vertical velocity, 28 to 31 ft/sec (8.5 to 9.4 m/sec); yaw, 0^0. All values are full scale.

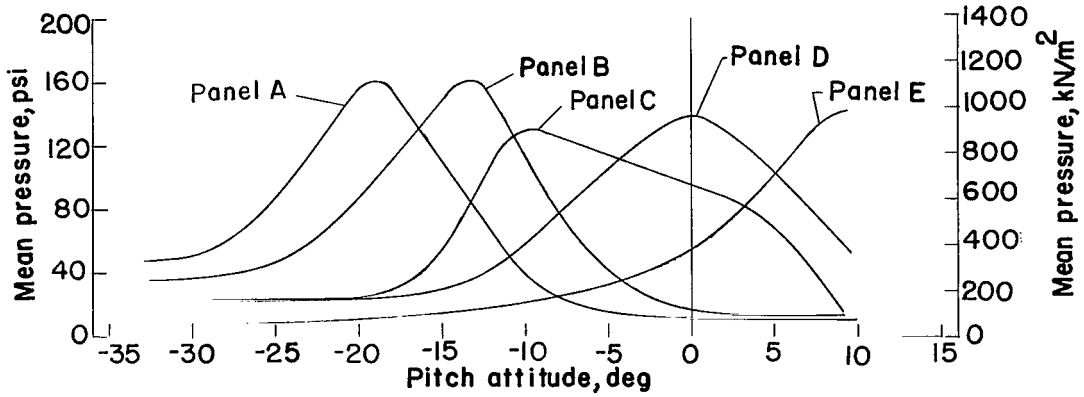

(a) Panels with area of 1.6 ft^2 (0.15 m^2).

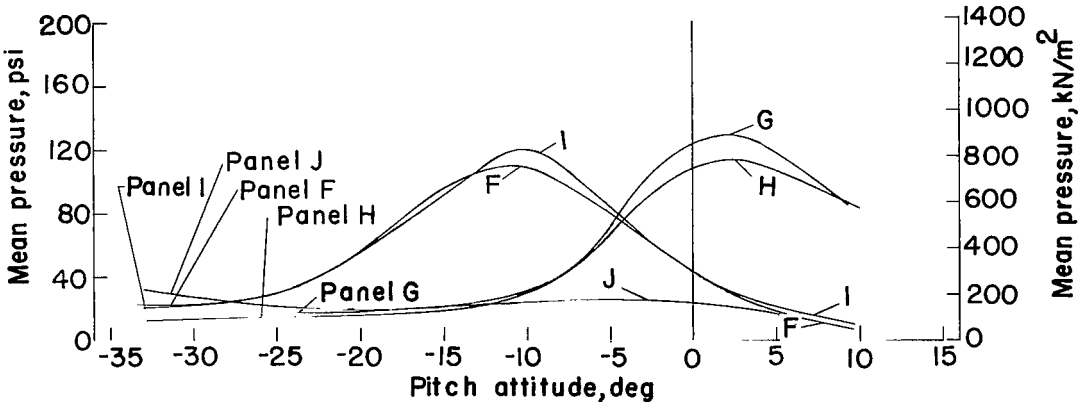

(b) Panels with area of 1.9 ft^2 (0.18 m^2).

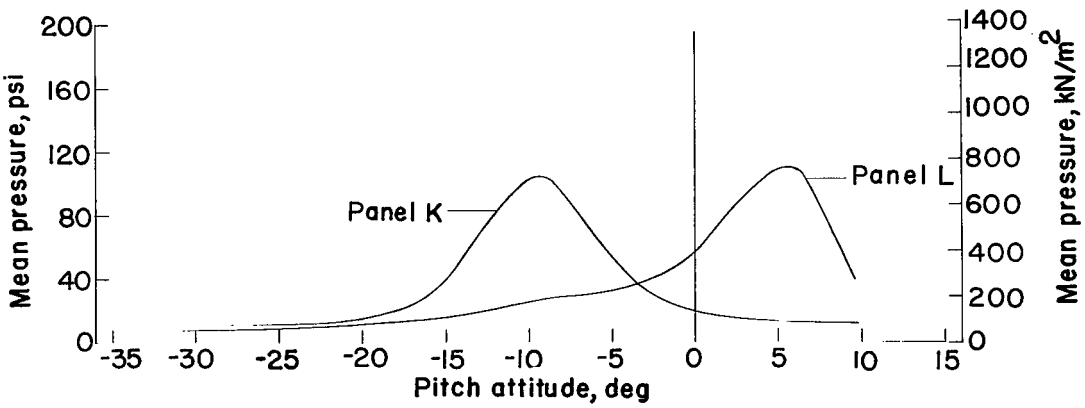

(c) Panels with area of 10.9 ft^2 (1.01 m^2).

Figure 19.- Fairings of panel-pressure data for vehicle at 180^0 roll. Vertical velocity, 28 to 31 ft/sec (8.5 to 9.4 m/sec); yaw, 0^0. All values are full scale.

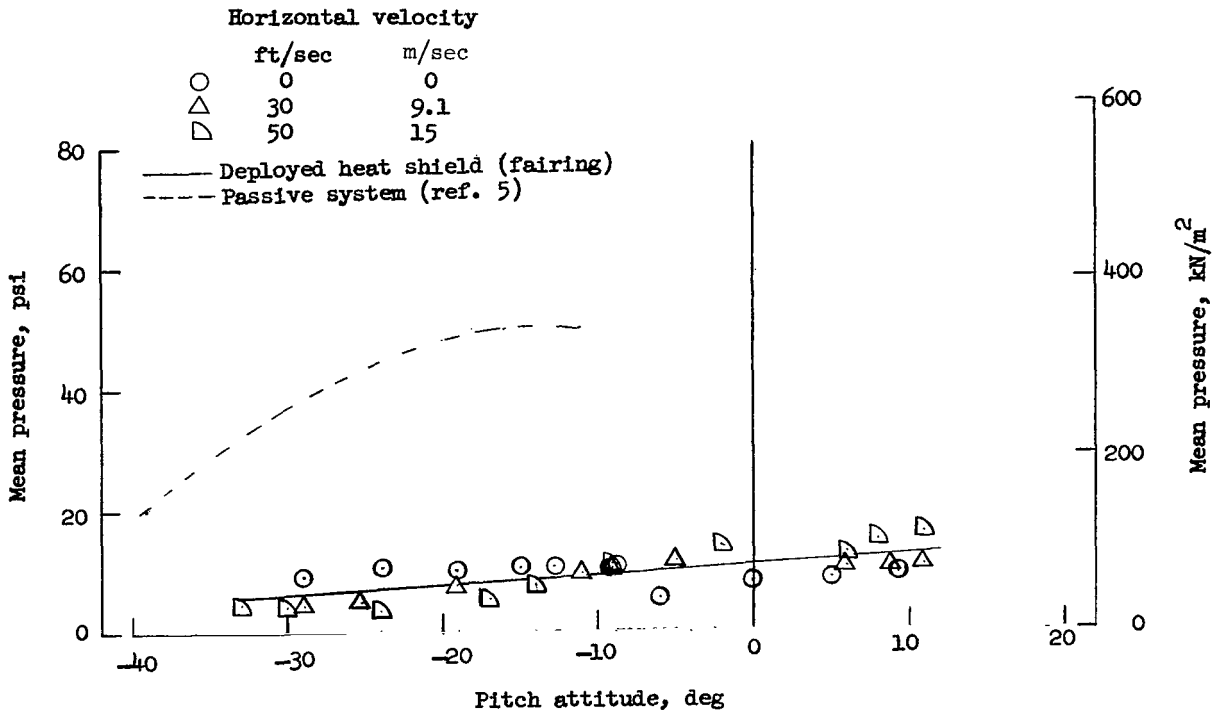

(a) Roll, 0°.

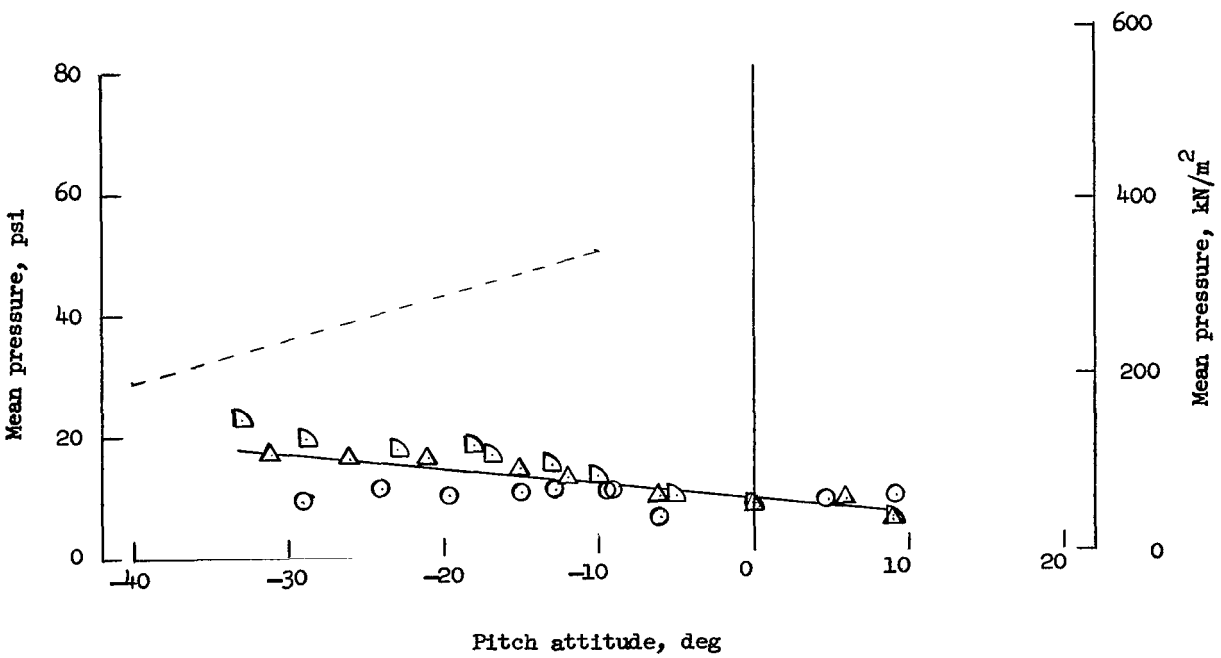

(b) Roll, 180°.

Figure 20.- Mean pressure at time of maximum acceleration. Vertical velocity, 28 to 31 ft/sec (8.5 to 9.4 m/sec); yaw, 0°. All values are full scale.

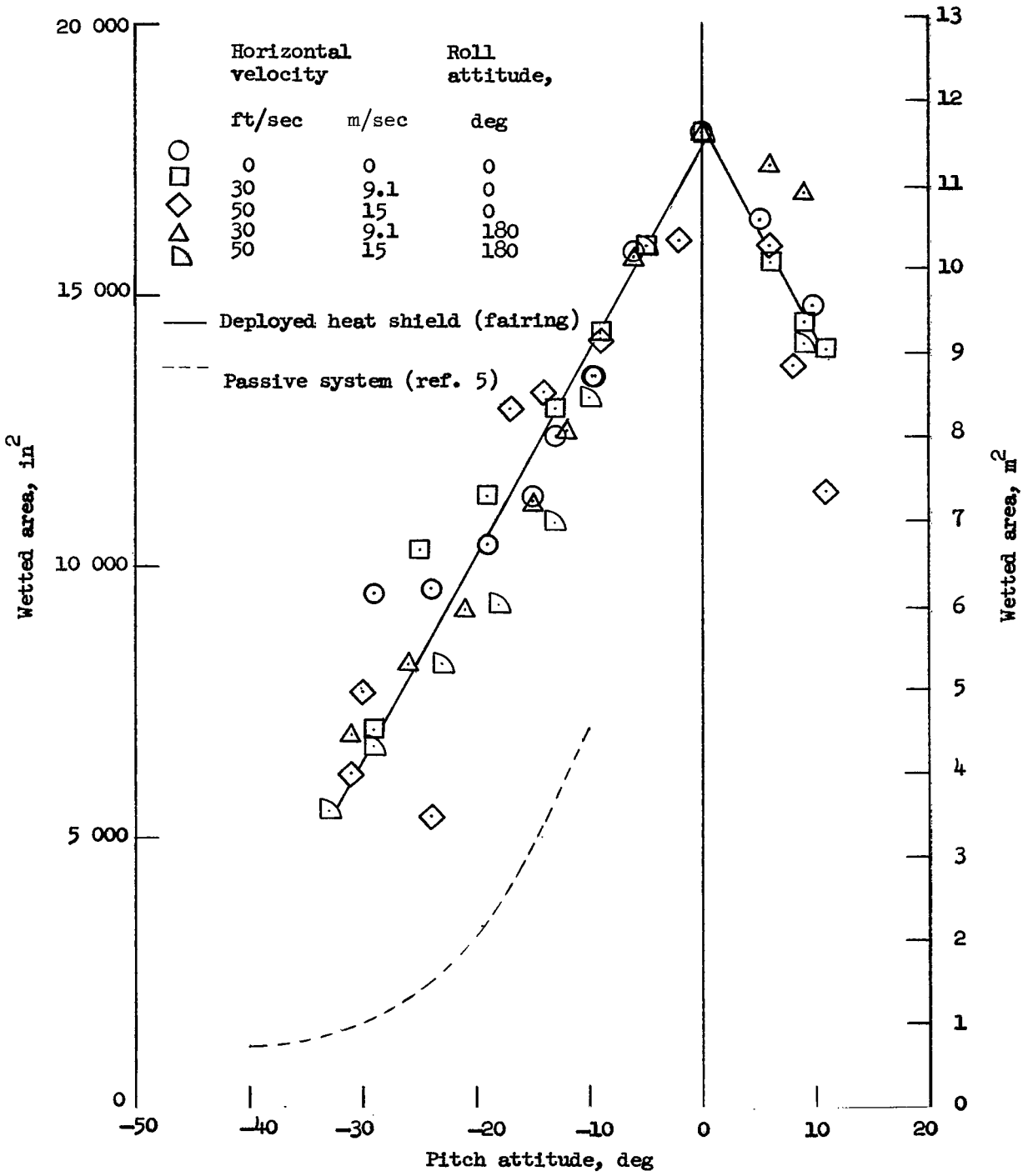

Figure 21.- Wetted area at time of maximum acceleration. Vertical velocity, 28 to 31 ft/sec (8.5 to 9.4 m/sec); yaw, 0^{0}. All values are full scale.

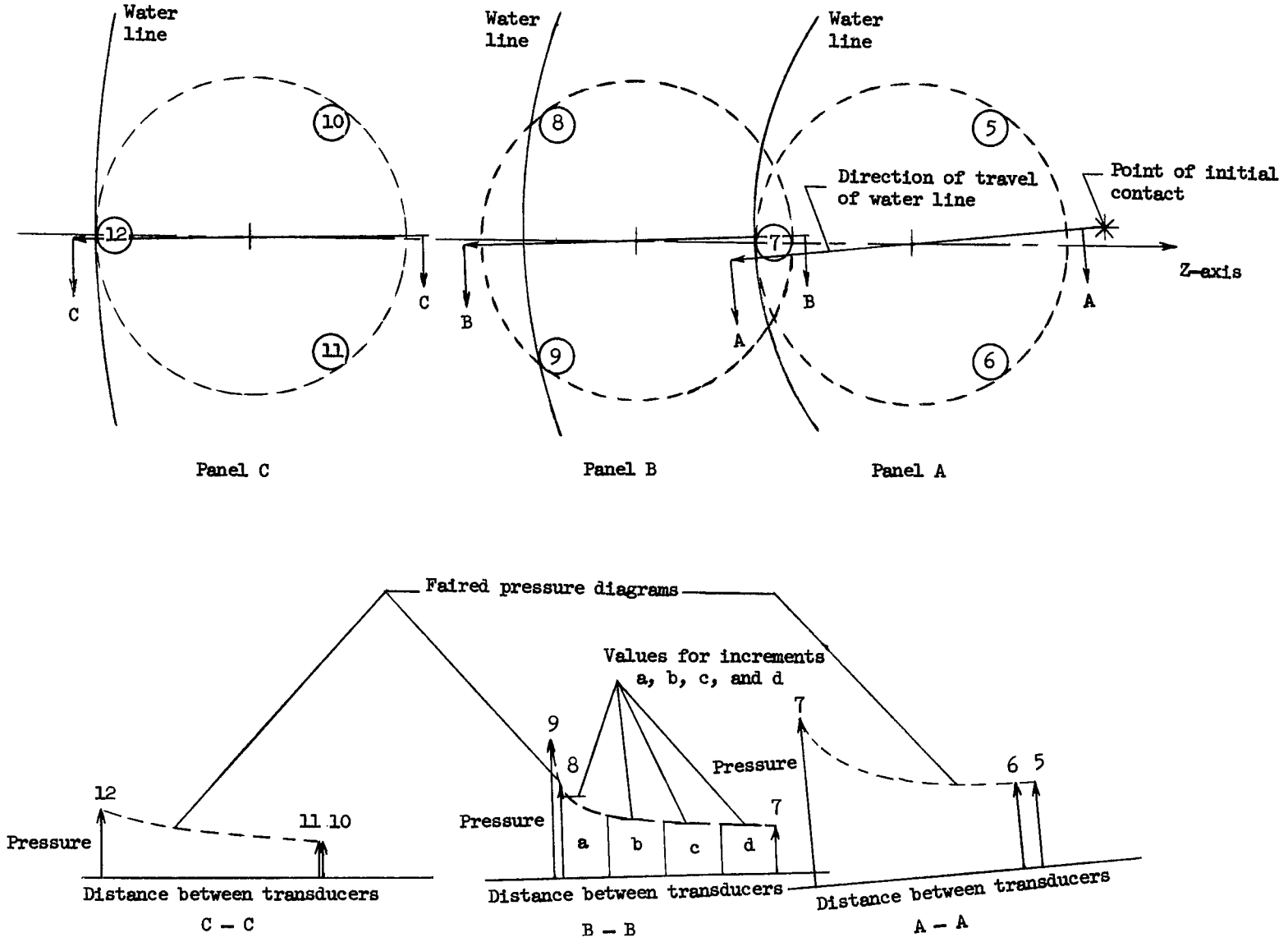

Figure 22.- Sketches of typical pressure panels to show method of obtaining mean pressures. Pressure diagram for panel B is divided into arbitrary increments a, b, c, and d.

A motion-picture film supplement L-980 is available on loan. Requests will be filled in the order received. You will be notified of the approximate date scheduled.

The film (16 mm, 4 min, color, silent) shows landing tests of the 1/4-scale model of the Apollo command module made on water using a deployed-heat-shield landing system.

Requests for the film should be addressed to:

Chief, Photographic Division
NASA Langley Research Center
Langley Station
Hampton, Va. 23365

CUT

Date _____

Please send, on loan, copy of film supplement L-980 to
TN D-4275

_____
Name of organization

_____
Street number

_____
City and State Zip code

Attention: Mr. _____

Title _____

"The aeronautical and space activities of the United States shall be conducted so as to contribute . . . to the expansion of human knowledge of phenomena in the atmosphere and space. The Administration shall provide for the widest practicable and appropriate dissemination of information concerning its activities and the results thereof."

—NATIONAL AERONAUTICS AND SPACE ACT OF 1958

NASA SCIENTIFIC AND TECHNICAL PUBLICATIONS

TECHNICAL REPORTS: Scientific and technical information considered important, complete, and a lasting contribution to existing knowledge.

TECHNICAL NOTES: Information less broad in scope but nevertheless of importance as a contribution to existing knowledge.

TECHNICAL MEMORANDUMS: Information receiving limited distribution because of preliminary data, security classification, or other reasons.

CONTRACTOR REPORTS: Scientific and technical information generated under a NASA contract or grant and considered an important contribution to existing knowledge.

TECHNICAL TRANSLATIONS: Information published in a foreign language considered to merit NASA distribution in English.

SPECIAL PUBLICATIONS: Information derived from or of value to NASA activities. Publications include conference proceedings, monographs, data compilations, handbooks, sourcebooks, and special bibliographies.

TECHNOLOGY UTILIZATION PUBLICATIONS: Information on technology used by NASA that may be of particular interest in commercial and other non-aerospace applications. Publications include Tech Briefs, Technology Utilization Reports and Notes, and Technology Surveys.

Details on the availability of these publications may be obtained from:

SCIENTIFIC AND TECHNICAL INFORMATION DIVISION

NATIONAL AERONAUTICS AND SPACE ADMINISTRATION

Washington, D.C. 20546